Optimization of the reload pattern for a nuclear reactor using perturbation theory

J.W. Koolwaaij

November, 1995

TU Delft
Technische Wiskunde en Informatica
Technische Universiteit Delft

Contents

Nomenclature

Independent variables

E	Energy	[MeV]
$\vec{r}$	Position	[cm]
t	Time	[s]
$\vec{\Omega}$	Direction	

Neutron transport

P	Power	[W]
Q	Neutron source	[cm^{-3} s^{-1}]
Q^*	Adjoint source	[†]
v	Neutron speed	[cm s^{-1}]
$\Phi(\vec{r}, E, \vec{\Omega}, t)$	Angular flux	[cm^{-2} s^{-1} MeV^{-1} sr^{-1}]
$\Phi^*(\vec{r}, E, \vec{\Omega}, t)$	Angular adjoint function	[cm [Q^*]]
χ	Neutron energy spectrum	[MeV^{-1}]
μ_f	Energy per fission	[MeV]
ν	Average number of emitted neutrons	
$\phi(\vec{r}, t)$	Scalar flux	[cm^{-2} s^{-1}]
$\phi^*(\vec{r}, t)$	Scalar adjoint function	[cm [Q^*]]

Cross sections

A	Nuclide mass relative to a neutron mass	
I	Neutron intensity	[cm^{-2} s^{-1}]
N_A	Constant of Avogadro	
R	Reaction rate	[cm^{-2} s^{-1}]
Σ_a	Macroscopic absorption cross section	[cm^{-1}]
Σ_c	Macroscopic capture cross section	[cm^{-1}]
Σ_f	Macroscopic fission cross section	[cm^{-1}]
Σ_s	Macroscopic scattering cross section	[cm^{-1}]
Σ_t	Macroscopic total cross section $= \Sigma_a + \Sigma_s$	[cm^{-1}]
Σ_{tr}	Macroscopic transport cross section $= \Sigma_a + (1 - \bar{\mu}_0)\Sigma_s$	[cm^{-1}]
μ_0	Cosine of the scattering angle	
ρ	Mass density	[kg m^{-3}]
σ_a	Microscopic absorption cross section	[b]‡
σ_c	Microscopic capture cross section	[b]

σ_f	Microscopic fission cross section	[b]
σ_s	Microscopic scattering cross section	[b]
σ_t	Microscopic total cross section	[b]
σ_{tr}	Microscopic transport cross section	[b]
Burnup		
$\mathbf{B}$	Burnup matrix	[s^{-1}]
$\vec{C}$	External source vector	[$\mathrm{cm}^{-3}\ \mathrm{s}^{-1}$]
$\mathbf{D}$	Decay matrix	[s^{-1}]
$\mathcal{N}_n^i$	Number of nuclides of type n in period T_i	
N_n^i	Nuclide density of type n in period T_i	[cm^{-3}]
$\vec{N}^i$	Nuclide density vector in period T_i	[cm^{-3}]
$\vec{N}_p^i$	Poison density vector in period T_i	[cm^{-3}]
$\mathbf{R}$	Microscopic cross section matrix	[b]
$\vec{\sigma}$	Microscopic cross section vector	[b]
γ	Fractional yield of the former nuclide per fission	
λ	Decay constant	[s^{-1}]
Eigenvalues		
k	Effective multiplication eigenvalue	
r	Boric acid volume factor	
α	Multiplication rate eigenvalue	[s^{-1}]
Miscellaneous		
$\vec{n}$	Outward normal on the boundary surface	
T	Period length	[s]
V	Volume	[cm^3]
V_{tot}	Total volume of the fuel element	[cm^3]
V_{mod}	Total volume of moderator in a fuel element	[cm^3]
V_{B}	Total volume of boric acid in a fuel element	[cm^3]

† The dimension of Q^* can be chosen freely.

‡ 1 barn $\hat{=}$ 10^{-24} cm^2. The name, coined by U.S. scientists, is derived from the proverbial phrase "side of a barn", something easy to hit.

Introduction

The core of a nuclear reactor contains a large number of fuel elements (uranium dioxide: UO_2). During operation, energy in the form of heat is extracted. The fissile material is consumed by fission and a number of fission products are formed. The core has to be refueled with fresh fuel once a year. Generally, not all the fuel is replaced, but only a fraction. When, for example, a fraction $1/n$ is replaced by fresh fuel, the core contains n age groups of fuel. The oldest fuel bundles are replaced by fresh fuel bundles. For optimal results a total redistribution of the different fuel elements is required. The description of this redistribution is called the reloading pattern. There too many possible reloading patterns to evaluate each one.

The aim of this research project is to provide a tool that can help in optimizing the reloading pattern. The adjoint equation is used in developing a method to quickly estimate the effects of a whole series of reloading patterns, patterns that are variations of one reloading pattern. The optimal variation can be varied again and so on until no improvement is possible.

The reloading pattern of a reactor can be optimal in a number of ways. Often, we want to produce as much energy as possible with the available fuel. Or, we want to use the oldest fuel batch as much as possible to decrease the amount of nuclear waste. So the objective function will be a weighted sum of energy costs, produced energy, burnup of the fuel elements, etc.

In chapter 1 a general description of the fission process inside a nuclear reactor core is given and reactor control is also treated. In chapter 2 the essential equations are introduced: the neutron transport equation and the burnup equations. Attention is paid to diffusion theory and homogenization of the cross sections. In chapter 3 the finite difference method to solve the diffusion equation is described. In chapter 4 the adjoint equation is introduced and with perturbation theory a fast forward algorithm is developed, which is described in chapter 5. To get an impression of the performance of this fast forward algorithm, we implemented the algorithm in MatLab, in chapter 6. The conclusions are given in the last chapter.

Key words: reactor physics, reloading patterns, perturbation theory, optimization

AMS(MOS) subject classifications: 81V35

Chapter 1

Nuclear fission

The fission process may be best understood through a consideration of the structure and stability of nuclear matter. Nuclides consist of nucleons (neutrons and protons), the total number of which is equal to the mass number of the nuclide. The actual mass of a nuclide is always less than the sum of the masses of the free neutrons and protons that constitute it, the difference being the mass equivalent of the energy of formation of the nuclide from it constituents. The conversion of mass to energy follows Einstein equation

$$E = mc^2, \tag{1.1}$$

where E is the energy equivalent of a mass, m, and c is the velocity of light. This difference is known as the mass defect and is a measure of the total binding energy (and, hence, the stability) of the nuclide. This binding energy is released during the formation of a nucleus from its constituent nucleons and would have to be supplied to the nuclide to decompose it into its individual nucleon components. A curve illustrating the average

Figure 1.1: The average binding energy per nucleon as a function of the mass number [16]

binding energy per nucleon as a function of the nuclear mass number is shown in figure 1.1. The largest binding energy (highest stability) occurs near mass number 56 (iron).

Figure 1.1 indicates energy can be produced by fusion of lighter nuclides or by fission of heavier nuclides. (See also [8])

In the fission process, a heavy nuclide such as uranium absorbs a neutron, after which it breaks up into two lighter nuclides. A substantial amount of energy is released simultaneously, as are several neutrons. These may then strike other heavy nuclides and cause them to fission. The continuous recurrence of this process results in a chain reaction (see figure 1.2) in which many billions of nuclides may fission within a small fraction of a second.

Figure 1.2: A simple schematic of a fission chain reaction [4]

1.1 Nuclear reactors

In a nuclear reactor such a self-sustaining series of fissions is carefully controlled, making it possible to utilize the enormous amount of energy released. This energy occurs in the form of radiation and the kinetic energy of the fission products expelled at high speeds. Much of it becomes thermal energy as the fission products come to rest. Some of the thermal energy is used to heat water and convert it to high-pressure steam. This steam drives a turbine, and the turbine's mechanical energy is then converted into electricity by means of a generator. Besides providing a valuable source of electric power for commercial use, nuclear reactors also serve to propel certain types of military surface vessels, submarines, and some unmanned spacecraft. Another major application of reactors is the production of radioactive isotopes that are used extensively in scientific research, medical therapy, and industry. These isotopes are created by bombarding nonradioactive substances with the neutrons released during fission.

Uranium
The only material occurring in nature that is readily fissionable and able to sustain a chain reaction is the uranium isotope ${}^{235}_{92}U$. It is a rare isotope; in natural uranium it is outnumbered roughly 140 to 1 by another isotope, ${}^{238}_{92}U$. When a single slow-moving

neutron collides with the nuclide of a $^{235}_{92}$U atom, the nuclide becomes suddenly so unstable that it splits into two major fragments and releases, on the average, two or three neutrons. Of these neutrons, at least one must succeed in producing another fission if the chain reaction is to persist. This is difficult to accomplish with natural uranium. Because its concentration of $^{235}_{92}$U nuclides is so small, the neutrons may escape the nuclear fuel without colliding with the fissionable nuclides, or they may strike the more plentiful $^{238}_{92}$U nuclides and be absorbed. To reduce the possibility of this happening, enriched uranium, which contains a higher percentage of $^{235}_{92}$U than does natural uranium, is often used instead of the latter as reactor fuel. Enrichment can be achieved by various processes, as, for example, gaseous diffusion. Since the energy from nuclear fuels would be limited if only $^{235}_{92}$U were utilized, reactors known as breeder reactors have been designed to convert nonfissionable uranium or other elements into fissionable isotopes.

Moderator

Most commercial power reactors of the conventional variety require a moderator to slow neutrons to a tiny fraction of their initial speed so as to increase their likelihood of causing fissions of $^{235}_{92}$U. Such substances as ordinary water (termed light water), deuterium oxide (heavy water), and graphite have been found to be effective moderators because they are able to slow down neutrons during the fission process without appreciably reducing their number by absorption.

Reactor control

Control of the rate at which neutrons are emitted, and thus of the reaction, is achieved by introducing materials, usually in the form of rods, that readily absorb slow neutrons. (See also section 1.2) Typically, rods made of cadmium or boron are gradually withdrawn from the reactor core until a chain reaction is initiated. They are reinserted into the core if the series of fissions begins to proceed at too great a rate, which would result in the release of an excessive amount of thermal energy and radiation and possibly cause meltdown of the core.

Coolant

The heat released by fission is removed from the reactor core by a coolant, either liquid or gaseous, that is circulated through the core. Desirable coolants have good heat-transfer properties as well as low neutron-absorbing properties. Both light water and heavy water have been employed, as have liquid metals (e.g., sodium), helium, and several other substances.

Shielding

As a chain reaction continues, fission products accumulate in the reactor core. Most of these fragments are intensely radioactive Consequently, the reactor must be surrounded by thick, heavy concrete shielding to protect operators and other individuals in the vicinity against radiation from these fragments and from that arising directly from the fission process itself.

Nuclear waste

The disposal of radioactive fission products and spent-fuel assemblies poses a more difficult problem than does the containment of radiation in the reactor core. Some of these nuclear wastes remain dangerously radioactive for thousands of years and thus must be eliminated or stored permanently. As yet, however, no practical method of safe and permanent disposal has been implemented. The algorithms presented in this report also try to minimize the amount of nuclear waste.

1.1.1 Light-water reactors

As noted above, LWRs are power reactors that are cooled and moderated with ordinary water. There are two basic types: the pressurized-water reactor (PWR) and the boiling-water reactor (BWR). In the first type, high-pressure, high-temperature water removes heat from the core and is then passed to a steam generator. Here the heat of the coolant is transferred to a stream of water in the generator (the secondary loop in figure 1.3B), causing the water to boil and slightly superheat. The steam generated by this serves as

Figure 1.3: Two reactor types: a BWR (A) and a PWR (B) [16]

the working fluid in a steam-turbine cycle.

In a boiling-water reactor, water passing through the core is allowed to boil at intermediate pressure, and the steam from the reactor is used directly in the power cycle (see figure 1.3A). Although the BWR seems simpler, the PWR has advantages with regard to fuel utilization and power density, and the two concepts have been economically competitive with each other since the 1960s. Both these light-water reactors are fueled with uranium dioxide pellets in zirconium alloy cladding. The BWR fuel is slightly less enriched, but the PWR fuel produces more energy before being discharged, and so these two aspects balance each other out economically. Because the BWR operates at lower pressure, it has a thinner pressure vessel than the PWR; however, because its power density is somewhat lower, the BWR's vessel has a larger diameter for the same reactor power. The internal system of a BWR is more complex, since there are internal recirculation pumps and complex steam separation and drying equipment within its vessel. Though the internals of the PWR are simpler, a BWR power plant is smaller because it has no steam generators. In fact, the steam generators -there are usually four of them in a big PWR plant- are larger than the reactor vessel itself. The control rods of a typical PWR are inserted from the top (through the reactor head), while those of a BWR are inserted from the bottom.

Light-water reactors are refuelled by removing the reactor head–after lowering and unlatching the safety rods in the case of a PWR. This exposes the reactor to visual observation. The pressure vessel is filled to the top with water, and, since the core is near the bottom of the vessel, the water acts as a shield for this operation. Then, the fuel assemblies to be removed are lifted up into a shielded cask within which they are transferred to a storage pool for cooling while they are still highly radioactive. Many of the remaining assemblies are then shifted within the core, and finally fresh fuel is loaded into the empty fuel positions. The purpose of shifting fuel at the time of reload is to achieve an optimal reactivity and power distribution for the next cycle of operation. Reloading is a time-consuming operation. In principle, it could be accomplished in three weeks, but in practice the plant undergoes maintenance during reload, which can take considerably more time–up to a few months. Maintenance and reload is scheduled during summer when electricity demand is lowest and the system usually has reserve capacity.

The discharged fuel stored in the storage pool is not only highly radioactive but also continues to produce energy. This energy is removed by natural circulation of the water in the storage pool. Originally it was expected that this spent fuel could be shipped out for reprocessing within two years, but this option is currently practiced only in France. In the United States, storage pools have continued to receive spent fuel, and some of the pools are filling up. Options available to nuclear plant operators are to store the spent fuel more densely than originally planned, to build new pools, or to store the oldest, no longer very hot fuel in above-ground silos (dry storage).

1.2 Reactor control

When a nuclear reactor is producing energy the average amount of neutrons should not increase (which would ultimately lead to a meltdown) or decrease (leading to a shutdown). So we want the reactor to have a constant average neutron population. Such a reactor is said to be critical. Criticality can be obtained by controlling the amount of neutron absorbing material in the core. The most frequently used absorbers are

1. Control rods

2. Burnable poison (e.g. ${}^{10}_{5}$B, ${}^{155}_{64}$Gd, ${}^{157}_{64}$Gd), built in the fissionable material

3. Boric acid (H_3BO_3), dissolved in the moderator or cooling fluid

A reactor is started up with a small neutron source and is temporarily in a supercritical state. The neutrons thus multiply and the power increases. When the desired power level is reached the reactor is made critical by adding neutron absorbers to the core, such that the neutron population becomes stable. The reactor cycle is finished when the core is critical without neutron absorbers and an increase of the average neutron density is not possible any more. Then the oldest fuel bundles are to be discharged, a shuffling scheme is applied and the vacancies in the core are filled with fresh fuel bundles.

1. Control rods
One of the methods for reactor control involves the use of special absorbing assemblies, namely, control rods or sometimes blades. Typically a reactor is equipped with three types of rods for different purposes:

a. Safety rods for starting up and shutting down the reactor,

b. Regulating rods for adjusting the reactor's power rate,

c. Shim rods for compensating for changes in reactivity as fuel is depleted by fission and capture.

The most important function of the safety rods is to shut down the reactor, either when such a shutdown is scheduled or in case of a real or suspected emergency. These rods contain enough absorber to terminate a chain reaction under any conceivable condition. They are withdrawn before fuel is loaded and remain available in case a loading error requires their action. After the fuel is loaded, the rods are inserted, to be withdrawn again when the reactor is ready for operation. The mechanism by which they are moved is designed to be fail-safe in the sense that if there is a mechanical failure the safety rods will fall by gravity into the reactor. In some cases, moreover, the safety rods have an automatic feature, such as a fuse, which releases them by virtue of physical effects independent of electronic signals.

Regulating rods are deliberately designed to affect reactivity only by a small degree. It is assumed that at some time the rods might be totally withdrawn by mistake, and the idea is to keep the added reactivity in such cases well within sensible limits. A well-designed regulating rod will add so little reactivity when it is removed that the delayed neutrons will continue to control the rate of power increase.

Shim rods are designed to compensate for the effects of burnup (i.e., energy production). Reactivity changes resulting from burnup can be large, but they occur slowly over periods of days to years, as compared to the seconds-to-minutes range over which safety actions and routine regulation take place. Therefore, shim rods may control a significant amount of reactivity, but they will work perfectly well under constraints on their speed of movement. A common way in which shims are operated is by inserting or removing them as regulating rods reach the end of their most useful position range. When this happens, shim rods are moved so that the regulating rods can be reset.

The functions of shim and safety rods are sometimes combined in rods that have low rates of withdrawal but that can be rapidly inserted. This is usually done when the effect of burnup is to decrease reactivity. The rods are only partially inserted at the outset of operation, but the reactor can be quickly shut down by lowering them all the way into the core (scramming). As operation proceeds, the rods are moved farther out so that there is a greater shutdown reactivity margin.

2. Burnable poison
The amount of shim control required can be reduced by the use of a burnable poison. This is a neutron-absorbing material, such as boron or gadolinium, which will burn off faster than the fissile material does. At the beginning of operation, this controls the extra reactivity that has been built into the fuel to compensate for the amount of fuel consumed. At the end of an operating period, the absorber material will have been almost completely destroyed by neutron capture.

3. Boric acid
In many cases, the coolant functions also as moderator, as in the case of light and heavy water. The moderator slows down the fast (high-energy) neutrons emitted in fission to speeds at which they are more likely to induce fission. In doing so, the moderator helps initiate and sustain a fission chain reaction. By varying the absorption cross section Σ_a of the moderator the reactivity of the reactor can be controlled. This variation is done by dissolving boric acid (H_3BO_3) into the moderator. Using boric acid has some advantages with respect to using control rods, because boric acid does not affect the homogeneity of the core.

Chapter 2

Forward calculations

In this chapter we examine the two central equations in nuclear reactor theory: the neutron transport equation describes the distribution of neutrons in the reactor, and the burnup equations describe the distribution of nuclides in the reactor. These two equations are coupled, because the neutron transport equation depends on the nuclide densities.

The cross sections form the link between these equations. Cross sections can be regarded as the probability per unit path length that a neutron will undergo a reaction.

2.1 Cross sections

The probability that a neutron-nuclide reaction will occur is characterized by a quantity called nuclear cross section. To define this quantity we consider a beam of neutrons, all traveling with the same speed and direction, which is incident normally and uniformly across the face of a target of material. Consider a target of one atomic layer thick, as in figure 2.1. Then the rate of neutron-nuclide reactions in the target will be proportional

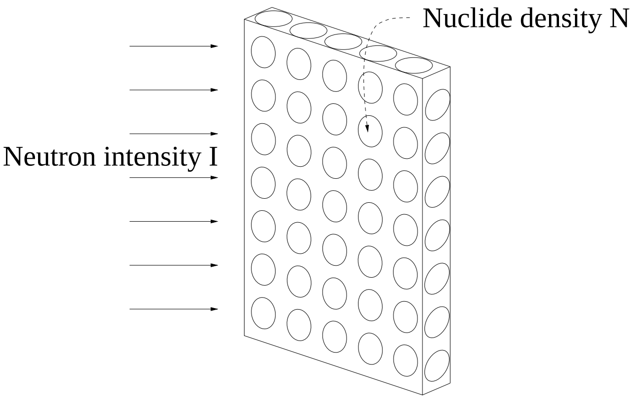

Figure 2.1: A neutron beam incident normally upon a thin target

to both the incident neutron beam intensity I and the number of target nuclides per unit

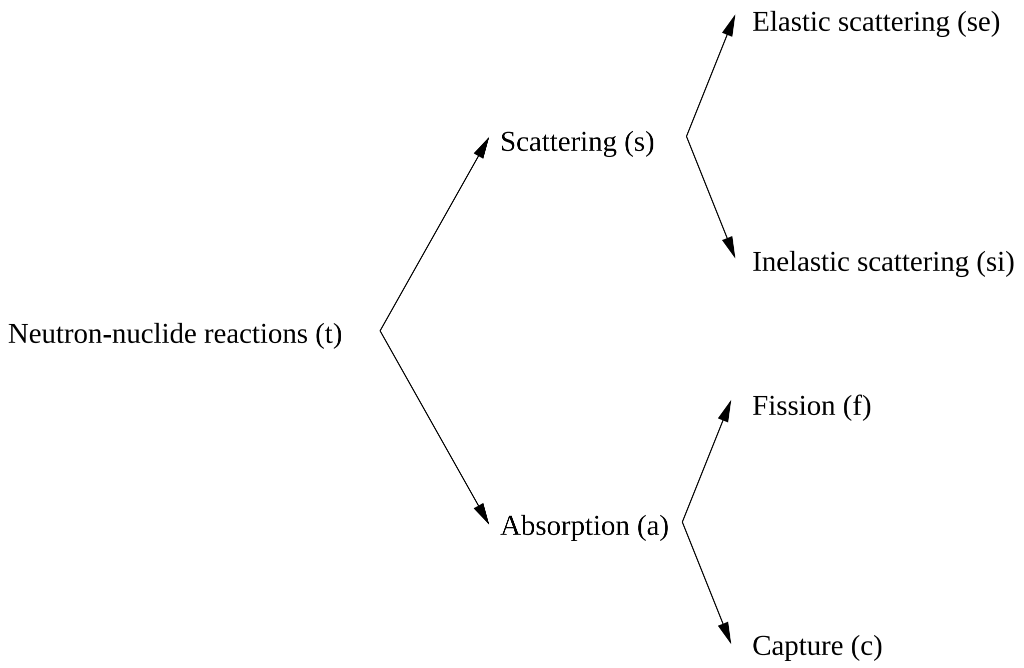

Figure 2.2: Neutron cross section hierarchy

area N_a. If we call the constant of proportionality σ, we can write the rate R at which the reactions occur per unit area on the target as

$$R = \sigma N_a I. \tag{2.1}$$

The constant σ, is known as the microscopic cross section characterizing the probability of a neutron-nuclide reaction for the nuclide. We might continue to think of σ as the effective cross sectional area presented by the nuclide to the beam of incident neutrons. Microscopic cross sections are usually measured in units of barns (b), where 1 barn is equal to 10^{-24} cm^2.

We can define a microscopic cross section for each type of neutron-nuclide reaction. For example, the appropriate cross sections characterizing absorption, fission and capture, are denoted by σ_a, σ_f and σ_c, respectively. And because cross sections are probabilities of various types of reactions

$$\sigma_a = \sigma_f + \sigma_c. \tag{2.2}$$

The sum of the cross sections for all possible reactions is known as the total cross section and denoted by σ_t,

$$\sigma_t = \sigma_a + \sigma_s = \sigma_f + \sigma_c + \sigma_{se} + \sigma_{si}. \tag{2.3}$$

To define the microscopic section σ we have considered a thin layer of nuclides. Now we want consider the neutron transmission through targets of more than one atomic layer thick (see figure 2.3). Let $I(x)$ be the the intensity of the non-interacted neutrons at any

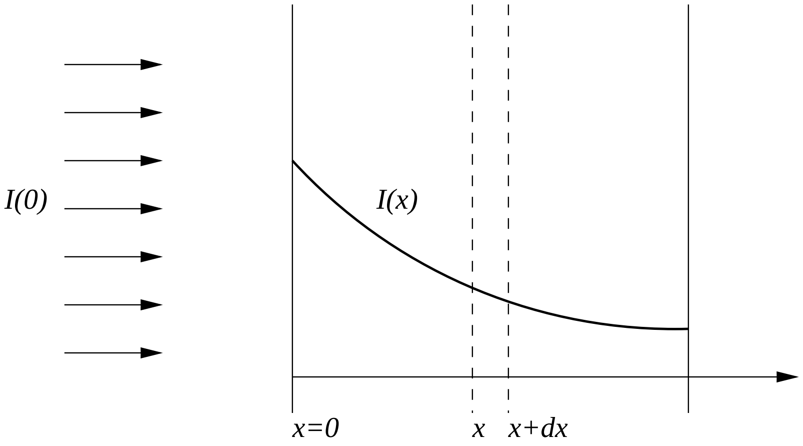

Figure 2.3: A neutron beam incident normally upon a thick target

point x in the target. In a thin layer of thickness dx the neutron intensity will decrease by the amount on neutrons interacting in that layer. So

$$-dI = \sigma N I dx, \tag{2.4}$$

where N is the nuclide density in the target. With the boundary condition $I(0) = I_0$ this equation can be solved

$$I(x) = I_0 \exp(-\sigma N x). \tag{2.5}$$

The product of the nuclide density N and the microscopic cross section σ is called the macroscopic cross section Σ

$$\Sigma = \sigma N. \tag{2.6}$$

Note that Σ is not really a cross section, since its units are inverse length. Σ can be interpreted as the probability per unit path length traveled that the neutron will undergo a neutron-nuclide reaction.

2.2 The neutron transport equation

In transport theory we consider a small volume in phase space $(V, E, \vec{\Omega})$ in the core, over which a neutron balance is constructed. For a description of the symbols see page 3. The change in time of the number of neutrons in $(V, E, \vec{\Omega})$ is caused by:

1. Fission of nuclides by neutrons, which produces on the average ν neutrons with energy spectrum χ.

2. Scattering of neutrons from $(E', \vec{\Omega}')$ to $(E, \vec{\Omega})$.

3. Flow of neutrons through the surface of V.

4. Interactions of neutrons with nuclides or control elements.

This balance is valid for any small volume in phase space $(V, E, \vec{\Omega})$ and now we can derive an exact equation for the angular flux Φ by simply balancing the various mechanisms by which neutrons can be gained or lost from an arbitrary volume V within the system [4].

$$\begin{aligned}
\frac{1}{v}\frac{\partial}{\partial t}\Phi(\vec{r}, E, \vec{\Omega}, t) &= \frac{\chi(E)}{4\pi}\int_0^\infty\int_{4\pi} \nu(E')\Sigma_f(\vec{r}, E', t)\Phi(\vec{r}, E', \vec{\Omega}', t)\, dE'\, d\Omega' \\
&+ \int_0^\infty\int_{4\pi} \Sigma_s(\vec{r}, E' \to E, \vec{\Omega}' \to \vec{\Omega}, t)\Phi(\vec{r}, E', \vec{\Omega}', t)\, dE'\, d\Omega' \\
&- \vec{\Omega} \cdot \nabla\Phi(\vec{r}, E, \vec{\Omega}, t) \\
&- \Sigma_t(\vec{r}, E, t)\Phi(\vec{r}, E, \vec{\Omega}, t).
\end{aligned} \tag{2.7}$$

The boundary condition is that there is no inward flow of neutrons through the boundary surface of the core:

$$\Phi(\vec{r}_b, E, \vec{\Omega}, t) = 0 \text{ for } \vec{n} \cdot \vec{\Omega} < 0 \tag{2.8}$$

with $\vec{n}$ the outward normal on the boundary surface.

2.3 Eigenvalue problems

It is difficult to include the control rods in the calculations because insertion of the control rods make the reactor core inhomogeneous, also in the third dimension. Even if the geometry has been modelled very accurately including the control rods, the model is rather sensitive to the control rods. So instead of trying to model the absorbers accurately, three different approaches can be taken to obtain criticality in the calculations:

1. Introducing k, the effective multiplication factor, in the fission term
2. Introducing α, the effective multiplication rate, in the time derivative of the neutron density
3. Introducing r, the volume factor of the extra absorbers, in the absorption term

Parameters k, α and r are eigenvalues such that the modelled flux is stationary. When the eigenvalue has been established, the behaviour of the reactor can be described by a stationary transport equation.

When we solve the flux Φ from this equation, we have one degree of freedom: Φ is determined up to a factor. This degree of freedom is used to bring the reactor at the desired power level. So the neutron flux density is normalized by the constant reactor power P:

$$\mu_f \int_V \int_0^\infty \int_{4\pi} \Sigma_f(\vec{r}, E, t)\Phi(\vec{r}, E, \vec{\Omega}, t)\, dV\, dE\, d\Omega = P \tag{2.9}$$

where μ_f is the energy per fission.

2.3.1 Effective multiplication factor

We introduce the effective multiplication factor k as a fictitious control parameter of the neutron production such that the neutron flux is stationary. The average number of emitted neutrons ν is then replaced by ν/k. So from the neutron transport equation 2.7 we derive the stationary transport equation with eigenvalue k:

$$\begin{aligned} 0 &= \frac{\chi(E)}{4\pi}\int_0^\infty \int_{4\pi} \frac{\nu(E')}{k}\Sigma_f(\vec{r},E')\Phi(\vec{r},E',\vec{\Omega}')\,dE'\,d\Omega' \\ &+ \int_0^\infty \int_{4\pi} \Sigma_s(\vec{r},E'\to E,\vec{\Omega}'\to\vec{\Omega})\Phi(\vec{r},E',\vec{\Omega}')\,dE'\,d\Omega' \\ &- \vec{\Omega}\cdot\nabla\Phi(\vec{r},E,\vec{\Omega}) \\ &- \Sigma_t(\vec{r},E)\Phi(\vec{r},E,\vec{\Omega}) \end{aligned} \tag{2.10}$$

with boundary condition 2.8.

In elementary reactor theory, k is thought of as a ratio between the total numbers of neutrons in successive generations. So to compute k numerically, we suppose a neutron source Q_1 at $t = 0$. We integrate the neutron transport equation 2.7 over time and define

$$\begin{aligned} \tilde{\Phi}_1(\vec{r},E,\vec{\Omega}) &= \int_0^\infty \Phi_1(\vec{r},E,\vec{\Omega},t)\,dt \\ \tilde{Q}_1(\vec{r},E,\vec{\Omega}) &= \int_0^\infty Q_1(\vec{r},E,\vec{\Omega},t)\,dt \end{aligned} \tag{2.11}$$

From this time integrated transport equation we solve $\tilde{\Phi}_1$. This first generation neutron flux forms the fission source for the second generation by

$$\tilde{Q}_2(\vec{r},E,\vec{\Omega}) = \frac{\chi(E)}{4\pi}\int_0^\infty \int_{4\pi} \nu(E')\Sigma_f(\vec{r},E')\tilde{\Phi}_1(\vec{r},E',\vec{\Omega}')\,dE'\,d\Omega' \tag{2.12}$$

As the foregoing procedure is iterated, it is to be expected that the angular flux in successive generations will increase for a supercritical system, decrease for a subcritical system, and become constant for a critical system. In any event, it is to expected that the ratio of fluxes in successive generations will approach a constant, independent of $\vec{r}$, $\vec{\Omega}$ and E. If this is so, then this constant is equal to k:

$$\frac{\int_V \int_0^\infty \int_{4\pi} \tilde{Q}_i\,dV\,dE\,d\Omega}{\int_V \int_0^\infty \int_{4\pi} \tilde{Q}_{i-1}\,dV\,dE\,d\Omega} = \text{constant} = k \tag{2.13}$$

2.3.2 Effective multiplication rate

Another way to simulate a reactor is to introduce an eigenvalue α that can be interpreted as a multiplication rate. Eigenvalue α is defined as the solution of the source-free, time-dependent neutron transport equation:

$$\frac{1}{v}\frac{\partial}{\partial t}\Phi(\vec{r},E,\vec{\Omega},t) = \frac{\alpha}{v}\Phi(\vec{r},E,\vec{\Omega},t) \tag{2.14}$$

This can be substituted into eq. 2.7 and we get

$$\begin{aligned}\frac{\alpha}{v}\Phi(\vec{r},E,\vec{\Omega}) &= \frac{\chi(E)}{4\pi}\int_0^\infty\int_{4\pi}\nu(E')\Sigma_f(\vec{r},E')\Phi(\vec{r},E',\vec{\Omega}')\,dE'\,d\Omega' \\ &+ \int_0^\infty\int_{4\pi}\Sigma_s(\vec{r},E'\to E,\vec{\Omega}'\to\vec{\Omega})\Phi(\vec{r},E',\vec{\Omega}')\,dE'\,d\Omega' \\ &- \vec{\Omega}\cdot\nabla\Phi(\vec{r},E,\vec{\Omega}) \\ &- \Sigma_t(\vec{r},E)\Phi(\vec{r},E,\vec{\Omega})\end{aligned} \tag{2.15}$$

with boundary condition 2.8.

We have defined α as the ratio of the time derivative of the neutron density and the neutron density. And α can also be computed with an iterative algorithm, a little more difficult than the one we used for the computation of k.

2.3.3 The boric acid volume factor

A volume V_B of boric acid is dissolved in a volume V_mod of moderator. The fuel element has a total volume of V_tot. So the new average cross section of a fuel element, which contains a fuel rod and moderator, becomes

$$\Sigma_a + \frac{V_\mathrm{B}}{V_\mathrm{tot}}(\Sigma_{a,\mathrm{B}} - \Sigma_{a,\mathrm{mod}}). \tag{2.16}$$

The eigenvalue r is defined as the volume of the boric acid in a fuel element divided by the total volume of that fuel element. So Σ_a is replaced by

$$\Sigma_a + r(\Sigma_{a,\mathrm{B}} - \Sigma_{a,\mathrm{mod}}), \quad 0 \le r \le \frac{V_\mathrm{mod}}{V_\mathrm{tot}}. \tag{2.17}$$

We substitute this new cross section into eq. 2.7

$$\begin{aligned}0 &= \frac{\chi(E)}{4\pi}\int_0^\infty\int_{4\pi}\nu(E')\Sigma_f(\vec{r},E')\Phi(\vec{r},E',\vec{\Omega}')\,dE'\,d\Omega' \\ &+ \int_0^\infty\int_{4\pi}\Sigma_s(\vec{r},E'\to E,\vec{\Omega}'\to\vec{\Omega})\Phi(\vec{r},E',\vec{\Omega}')\,dE'\,d\Omega' \\ &- \vec{\Omega}\cdot\nabla\Phi(\vec{r},E,\vec{\Omega}) \\ &- \left[\Sigma_t(\vec{r},E) + r(\Sigma_{a,\mathrm{B}} - \Sigma_{a,\mathrm{mod}})\right]\Phi(\vec{r},E,\vec{\Omega}),\end{aligned} \tag{2.18}$$

again with boundary condition 2.8.

2.4 Solving the quasi-stationary equation

Because of exhaustion of the fuel rods, the macroscopic cross sections vary in time. Therefore the time is divided into periods $T_i = \{t|(i-1)T < t < iT\}, i = 1,\ldots,n$ (with T

the length of the period). The flux density and cross sections are assumed to be constant during a period T_i:

$$\Phi^i(\vec{r}, E, \vec{\Omega}) = \Phi(\vec{r}, E, \vec{\Omega}, t)|_{t \in T_i} \text{ and } \Sigma^i(\vec{r}, E, \vec{\Omega}) = \Sigma(\vec{r}, E, \vec{\Omega}, t)|_{t \in T_i} \tag{2.19}$$

Let $t \in T_i$ and substitute expressions 2.19 into the stationary equation 2.10 with for example the multiplication factor k:

$$\begin{aligned} 0 &= \frac{\chi(E)}{4\pi} \int_0^\infty \int_{4\pi} \frac{\nu(E')}{k^i} \Sigma_f^i(\vec{r}, E') \Phi^i(\vec{r}, E', \vec{\Omega}')\, dE'\, d\Omega' \\ &+ \int_0^\infty \int_{4\pi} \Sigma_s^i(\vec{r}, E' \to E, \vec{\Omega}' \to \vec{\Omega}) \Phi^i(\vec{r}, E', \vec{\Omega}')\, dE'\, d\Omega' \\ &- \vec{\Omega} \cdot \nabla \Phi^i(\vec{r}, E, \vec{\Omega}) \\ &- \Sigma_t^i(\vec{r}, E) \Phi^i(\vec{r}, E, \vec{\Omega}) \end{aligned} \tag{2.20}$$

with boundary condition

$$\Phi^i(\vec{r}_b, E, \vec{\Omega}) = 0 \text{ for } \vec{n} \cdot \vec{\Omega} < 0 \tag{2.21}$$

In sections 2.4.1 - 2.4.4 we describe four methods to solve the equation.

2.4.1 Diffusion theory

In the discussion concerning reloading patterns we are mainly interested in the power distribution in the reactor and power is only a function of $\vec{r}$ and t. So we use the one-group diffusion theory ($1\frac{1}{2}$-group theory is treated in the next session) and assume that

1. the cross sections are independent of neutron energy, or suitable weighted cross sections over energy are used.
2. the medium is isotropic, in the sence that the scattering angle of the neutrons is independent of the incoming direction.

In this approach we use the scalar flux ϕ instead of the angular flux Φ. Those two fluxes are related by

$$\phi(\vec{r}) = \int_{4\pi} \int_0^\infty \Phi(\vec{r}, E, \vec{\Omega})\, dE\, d\Omega \tag{2.22}$$

Integration of eq. 2.20 over all energies E and over all directions $\vec{\Omega}$ gives

$$\int_{4\pi} \vec{\Omega} \cdot \nabla \Phi^i(\vec{r}, \vec{\Omega})\, d\Omega - \left(\frac{\nu}{k^i} \Sigma_f^i(\vec{r}) - \Sigma_t^i(\vec{r}) + \Sigma_s^i(\vec{r}) \right) \phi^i(\vec{r}) = 0 \tag{2.23}$$

and with $\Sigma_a^i = \Sigma_t^i - \Sigma_s^i$, we get

$$\int_{4\pi} \vec{\Omega} \cdot \nabla \Phi^i(\vec{r}, \vec{\Omega})\, d\Omega - \left(\frac{\nu}{k^i} \Sigma_f^i(\vec{r}) - \Sigma_a^i(\vec{r}) \right) \phi^i(\vec{r}) = 0. \tag{2.24}$$

In diffusion theory, $\Phi^i(\vec{r},\vec{\Omega})$ is approximated by spherical harmonic functions:

$$\Phi^i(\vec{r},\vec{\Omega}) \doteq \frac{1}{4\pi}\left(\phi^i(\vec{r}) + 3\vec{\Omega}\cdot\int_{4\pi}\vec{\Omega}\,\Phi^i(\vec{r},\vec{\Omega})\,d\Omega\right). \tag{2.25}$$

This approximation yields, when substituted into eq. 2.20:

$$\int_{4\pi}\vec{\Omega}\,\Phi^i(\vec{r},\vec{\Omega})\,d\Omega = -\frac{1}{3\Sigma^i_{tr}(\vec{r})}\nabla\phi^i(\vec{r}), \tag{2.26}$$

where the transport cross section is defined as

$$\Sigma^i_{tr}(\vec{r}) = \Sigma^i_a(\vec{r}) + (1-\overline{\mu}_0(\vec{r}))\Sigma^i_s(\vec{r}), \tag{2.27}$$

and $\overline{\mu}_0$ is the average value of the cosine of the scattering angle (angle between incoming and scattered direction). Substitution of eq. 2.26 into eq. 2.24 gives the diffusion equation for the scalar flux ϕ

$$\nabla\cdot\frac{1}{3\Sigma^i_{tr}(\vec{r})}\nabla\phi^i(\vec{r}) + \left(\frac{\nu}{k^i}\Sigma^i_f(\vec{r}) - \Sigma^i_a(\vec{r})\right)\phi^i(\vec{r}) = 0. \tag{2.28}$$

We assume that the inward neutron flow through the boundary surface is equal to zero (see eq. 2.8). For all points $\vec{r}_b$ on the boundary surface, we get the condition

$$\phi^i(\vec{r}_b) + \frac{2}{3\Sigma^i_{tr}(\vec{r}_b)}\,\vec{n}\cdot\nabla\phi^i(\vec{r}_b) = 0. \tag{2.29}$$

The diffusion equation is solved using a finite difference or finite element scheme (see chapter 3).

2.4.2 $1\frac{1}{2}$-group diffusion theory

Neutrons produced by fission have a very high energy (about 2 MeV). This neutron energy is reduced to about 1 eV mainly by scattering in the moderator. When a neutron has an energy below 1 eV, its interaction probabilities with the fissionable material are much larger than above 1 eV. So we consider two energy groups:

1. neutrons with an energy above 1 eV: fast neutrons
2. neutrons with an energy below 1 eV: thermal neutrons

As said, neutrons produced by fission are in group 1 and neutrons are transferred by scattering from group 1 to group 2. So we get two equations: one for the fast and one for the thermal neutron flux.

$$\begin{aligned}
\Sigma_s^{1\to 2}(\vec{r})\phi^1(\vec{r}) &= \nabla\cdot\frac{1}{3\Sigma^1_{tr}(\vec{r})}\nabla\phi^1(\vec{r}) + \frac{1}{k}\left(\nu\Sigma^1_f(\vec{r})\phi^1(\vec{r}) + \nu\Sigma^2_f(\vec{r})\phi^2(\vec{r})\right) - \Sigma^1_a(\vec{r})\phi^1(\vec{r}) \\
-\Sigma_s^{1\to 2}(\vec{r})\phi^1(\vec{r}) &= \nabla\cdot\frac{1}{3\Sigma^2_{tr}(\vec{r})}\nabla\phi^2(\vec{r}) - \Sigma^2_a(\vec{r})\phi^2(\vec{r})
\end{aligned} \tag{2.30}$$

It appears that for light water reactors the ratio of the thermal neutron diffusion and the thermal absorption is about 5×10^{-4}. So in a light water reactor, only fast neutrons are important for neutron diffusion. If we neglect the thermal neutron diffusion term $\nabla \cdot \nabla \phi^2$, we get

$$\phi^2(\vec{r}) = \frac{\Sigma_s^{1\to 2}(\vec{r})}{\Sigma_a^2(\vec{r})}\phi^1(\vec{r}) \tag{2.31}$$

If we substitute this into the first equation of 2.30, it follows that

$$\nabla \cdot \frac{1}{3\Sigma_{tr}^1(\vec{r})}\nabla\phi^1(\vec{r}) + \left(\frac{1}{k}\left(\nu\Sigma_f^1(\vec{r}) + \nu\Sigma_f^2(\vec{r})\frac{\Sigma_s^{1\to 2}(\vec{r})}{\Sigma_a^2(\vec{r})}\right) - \Sigma_s^{1\to 2}(\vec{r}) - \Sigma_a^1(\vec{r})\right)\phi^1(\vec{r}) = 0 \tag{2.32}$$

So with the assumption that the diffusion of the thermal neutrons can be neglected, the two equations (2.30) reduce to one equation (2.32) for the fast neutron flux. This is why this method is called the $1\frac{1}{2}$-group diffusion theory. The thermal neutron flux can then simply be computed with eq. 2.31.

For brevity reasons the one-group diffusion equation is used in the next sections. If you prefer using the $1\frac{1}{2}$-group diffusion equation simply replace in the neutron transport equation

$$\phi(\vec{r}) \quad \text{by} \quad \phi^1(\vec{r}), \tag{2.33}$$

$$\Sigma_\diamond(\vec{r}) \quad \text{by} \quad \Sigma_\diamond^1(\vec{r}) + \Sigma_\diamond^2(\vec{r})\frac{\Sigma_s^{1\to 2}(\vec{r})}{\Sigma_a^2(\vec{r})} \text{ for } \diamond \in \{a, c, f, s, tr\}, \tag{2.34}$$

$$\sigma_\diamond(\vec{r}) \quad \text{by} \quad \sigma_\diamond^1(\vec{r}) + \sigma_\diamond^2(\vec{r})\frac{\Sigma_s^{1\to 2}(\vec{r})}{\Sigma_a^2(\vec{r})} \text{ for } \diamond \in \{a, c, f, s, tr\}. \tag{2.35}$$

The total flux is the sum of the thermal and the fast flux

$$\phi(\vec{r}) = \left(1 + \frac{\Sigma_s^{1\to 2}(\vec{r})}{\Sigma_a^2(\vec{r})}\right)\phi^1(\vec{r}). \tag{2.36}$$

2.4.3 Discrete ordinate methods

In the discrete ordinate approach, we would first represent the independent direction variable $\vec{\Omega}$ by a discrete set of N directions $\vec{\Omega}_n, n = 1, \ldots, N$. We then represent functions of $\vec{\Omega}$ by their fluxes in these directions:

$$f(\vec{\Omega}) \to f(\vec{\Omega}_n) \equiv f_n, \quad n = 1, \ldots, N \tag{2.37}$$

In such a discrete ordinate treatment of angle, the integral of $\vec{\Omega}$ becomes a summation:

$$\int_{4\pi} \Phi^i(\vec{r}, \vec{\Omega})\, d\Omega = \sum_{n=1}^{N} w_n \Phi^i(\vec{r}, \vec{\Omega}_n) \tag{2.38}$$

where w_n are approximately chosen quadrature weights for the particular numerical integration scheme used to handle the angular integrals. When we assume isotropic scattering, the transport equation 2.20 reduces to a coupled set of N equations:

$$\vec{\Omega}_n \cdot \nabla\Phi_n^i(\vec{r}) + \Sigma_t^i(\vec{r})\Phi_n^i(\vec{r}) = \frac{1}{4\pi}\left(\frac{\nu}{k}\Sigma_f^i(\vec{r}) + \Sigma_s^i(\vec{r})\right)\sum_{m=1}^{N} w_m \Phi_m^i(\vec{r}). \tag{2.39}$$

These equations are commonly referred to as the S_N equations.

2.4.4 The Monte Carlo method

The Monte Carlo method is a numerical procedure based on probability theory. In neutron transport calculations, Monte Carlo techniques are applicable, because a cross section may be interpreted as a probability of interaction per unit distance traveled by a neutron. Thus, a set of neutron histories is generated by following individual, random neutrons through successive collisions. The locations of the actual collisions and the result of such collisions are sampled from their probability distributions using sets of random numbers.

2.5 The burnup equations

All heavy nuclides can split if they are in an excited enough state, but only a few split readily when struck by slow (low-energy) neutrons. Such species of atoms are called fissile. The most important of these are ${}^{233}_{92}\mathrm{U}$, ${}^{235}_{92}\mathrm{U}$, ${}^{239}_{94}\mathrm{Pu}$ and ${}^{241}_{94}\mathrm{Pu}$. The only one that occurs in usable amounts in nature is ${}^{235}_{92}\mathrm{U}$, which makes up a mere 0.712 percent of natural uranium by weight. ${}^{233}_{92}\mathrm{U}$ can be produced by neutron capture in natural thorium (${}^{232}_{90}\mathrm{Th}$); that is to say, when a nuclide of ${}^{232}_{90}\mathrm{Th}$ absorbs a neutron, it becomes ${}^{233}_{92}\mathrm{U}$. Similarly, ${}^{239}_{94}\mathrm{Pu}$ is created by neutron capture in ${}^{238}_{92}\mathrm{U}$ (the principal constituent of naturally occurring uranium), and ${}^{241}_{94}\mathrm{Pu}$ is formed when a neutron is absorbed into ${}^{240}_{94}\mathrm{Pu}$ (${}^{240}_{94}\mathrm{Pu}$ builds up over time in most power reactors). ${}^{232}_{90}\mathrm{Th}$, ${}^{238}_{92}\mathrm{U}$ and ${}^{240}_{94}\mathrm{Pu}$ are termed fertile materials because they can be transformed into fissile materials.

A power reactor contains both fissile and fertile materials. The fertile materials replace fissile materials that are destroyed by fission. This permits the reactor to run longer before the amount of fissile material decreases to the point where criticality can no longer be maintained.

In this section we want to compute the nuclide densities N^{i+1} in period T_{i+1}, when N^i is known. Let $N_n(\vec{r},t)$ be the nuclide density of type n and $\vec{N}$ the nuclide density vector, which is defined by

$$\vec{N}(\vec{r},t) = [N_1(\vec{r},t), N_2(\vec{r},t), \dots, N_n(\vec{r},t)]^{\mathrm{T}} \tag{2.40}$$

The rate at which $\vec{N}$ changes in time is equal to

$$\frac{d\vec{N}}{dt} = \phi(\vec{r},t)\mathbf{R}(\sigma)\vec{N}(\vec{r},t) + \mathbf{D}(\lambda)\vec{N}(\vec{r},t) + \vec{C}(\vec{r},t), \tag{2.41}$$

where $\mathbf{R}$ is the cross section matrix, $\mathbf{D}$ the decay matrix and $\vec{C}$ an external source of nuclides.

2.5.1 Time dependent nuclide densities

The behaviour of the reactor is dominated by the concentrations of two isotopes of uranium (${}^{235}_{92}\mathrm{U}$, ${}^{238}_{92}\mathrm{U}$) and plutonium (${}^{239}_{94}\mathrm{Pu}$), denoted by N_5, N_8 and N_9. All three nuclides have an insignificant decay rate and there is no external source. The number of interactions per unit volume and time is equal to $\Sigma\phi$, where Σ is the cross section of that particular interaction. The macroscopic cross sections is related to the microscopic cross sections by

$$\Sigma = \sigma N. \tag{2.42}$$

So the nuclide densities can be calculated by solving the following system of burnup equations

$$\frac{d}{dt}\vec{N}(\vec{r},t) = \phi(\vec{r},t)\mathbf{R}(\sigma)\vec{N}(\vec{r},t) = \mathbf{B}(\vec{r},t)\vec{N}(\vec{r},t), \tag{2.43}$$

where the burnup matrix $\mathbf{B}(\vec{r},t)$ is defined as

$$\mathbf{B}(\vec{r},t) = \begin{bmatrix} -\sigma_{a5}\phi(\vec{r},t) & & \\ & -\sigma_{c8}\phi(\vec{r},t) & \\ & \sigma_{c8}\phi(\vec{r},t) & -\sigma_{a9}\phi(\vec{r},t) \end{bmatrix} \tag{2.44}$$

and the nuclide vector $\vec{N}(\vec{r},t)$ as

$$\vec{N}(\vec{r},t) = \begin{bmatrix} N_5(\vec{r},t) \\ N_8(\vec{r},t) \\ N_9(\vec{r},t) \end{bmatrix}. \tag{2.45}$$

So by this relation the neutron flux fields and the nuclide density fields are coupled, and hence time dependence in the nuclide densities induces time dependence in the neutron flux distribution.

We make use of the quasi-static approach in which the neutron flux is kept stationary during a period T_i, where T_i is sufficiently small (e.g. 2 weeks) with respect to the cycle length of one year. In the quasi-static approach we thus get the following form of the burnup equations

$$\frac{d}{dt}\vec{N}(\vec{r},t) = \mathbf{B}^i(\vec{r})\vec{N}(\vec{r},t) \text{ for } t \in T_i, \tag{2.46}$$

where the quasi-static burnup matrix $\mathbf{B}^i$ is defined as

$$\mathbf{B}^i(\vec{r}) = \begin{bmatrix} -\sigma_{a5}\phi^i(\vec{r}) & 0 & 0 \\ 0 & -\sigma_{c8}\phi^i(\vec{r}) & 0 \\ 0 & \sigma_{c8}\phi^i(\vec{r}) & -\sigma_{a9}\phi^i(\vec{r}) \end{bmatrix}. \tag{2.47}$$

This system can easily be solved and if the nuclide density $\vec{N}$ at $t = iT$ is known we can compute $\vec{N}$ at $t = iT + T$ by

$$\vec{N}(\vec{r}, iT + T) = \exp(\mathbf{B}^i T)(\vec{r})\vec{N}(\vec{r}, iT). \tag{2.48}$$

And in our quasi-static notation $\vec{N}^i(\vec{r}) = \vec{N}(\vec{r}, iT)$ we get

$$\vec{N}^{i+1}(\vec{r}) = \exp(\mathbf{B}^i T)(\vec{r})\vec{N}^i(\vec{r}), \tag{2.49}$$

where $\exp(\mathbf{B}^i T)$ is the matrix

$$\begin{bmatrix} \exp(-\sigma_{a5}\phi^i T) & 0 & 0 \\ 0 & \exp(-\sigma_{c8}\phi^i T) & 0 \\ 0 & \frac{\sigma_{c8}}{\sigma_{a9}-\sigma_{c8}}(\exp(-\sigma_{c8}\phi^i T) - \exp(-\sigma_{a9}\phi^i T)) & \exp(-\sigma_{a9}\phi^i T) \end{bmatrix}. \quad (2.50)$$

Note that the space dependence is omitted here.

Example
At time $t = 0$ a reactor with 14×14 elements is refuelled with fresh fuel (5% enriched uranium), as in figure 2.4. The darker positions are filled with fuel and the lighter only

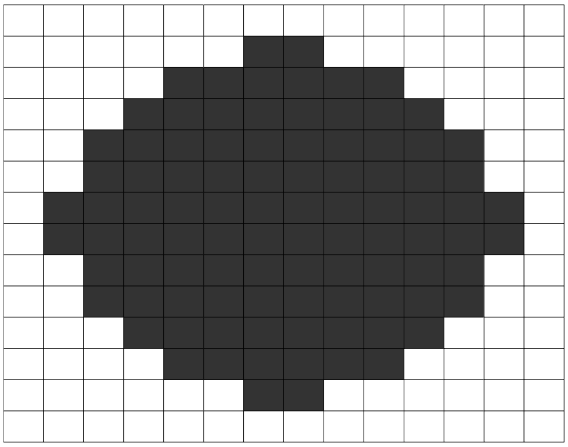

Figure 2.4: ${}^{235}_{92}$U density at $t = 0$

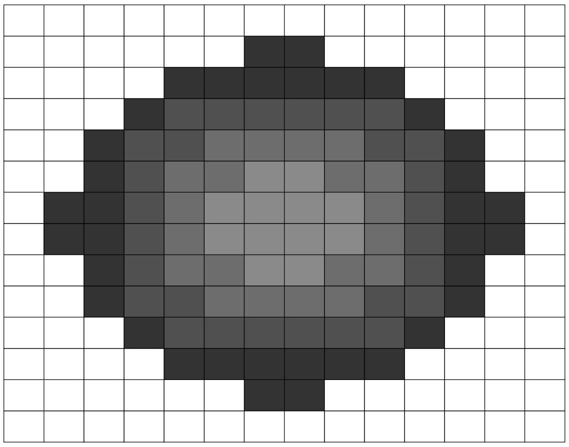

Figure 2.5: ${}^{235}_{92}$U density at $t = 360$

with moderator. The initial nuclide density vector is then in all fuel elements $\vec{N}^0 = [3.35 \cdot 10^{-4}\text{cm}^{-3}, 6.356 \cdot 10^{-3}\text{cm}^{-3}, 1.00 \cdot 10^{-12}\text{cm}^{-3}]^{\text{T}}$. With BoldVenture we calculate the nuclide densities in the reactor again after a cycle time of 360 days. The result is shown in figure 2.5. Lighter fuel elements have a higher burnup. In the center of the core the burnup is higher, because the flux has a maximum there (see figures 2.6 and 2.7).

2.5.2 Reactor poisons

The reactor poisons ${}^{135}_{54}$Xe are produced as byproducts in the fission process and ${}^{149}_{62}$Sm have a significant influence on the behaviour of the reactor because of their very large absorption cross sections. ^{135}Xe is a decay product and a fission product:

$$\overset{\gamma=3.3\%}{\downarrow}\; \overset{3.1\%}{\downarrow} \; \overset{0.25\%}{\downarrow}$$
$${}^{135}_{52}\text{Te} \xrightarrow{19.2\text{s}} {}^{135}_{53}\text{I} \xrightarrow{6.6\text{h}} {}^{135}_{54}\text{Xe} \xrightarrow{9.2\text{h}} \dots \quad (2.51)$$

and ^{149}Sm is a decay product:

$$\overset{\gamma=1.09\%}{\downarrow}$$
$${}^{149}_{60}\text{Nd} \xrightarrow{1.73\text{h}} {}^{149}_{61}\text{Pm} \xrightarrow{53.1\text{h}} {}^{149}_{62}\text{Sm}. \quad (2.52)$$

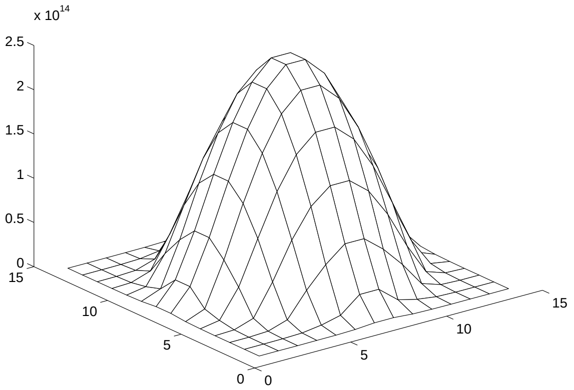

Figure 2.6: Fast flux (averaged over cycle time) [cm^{-2} s^{-1}]

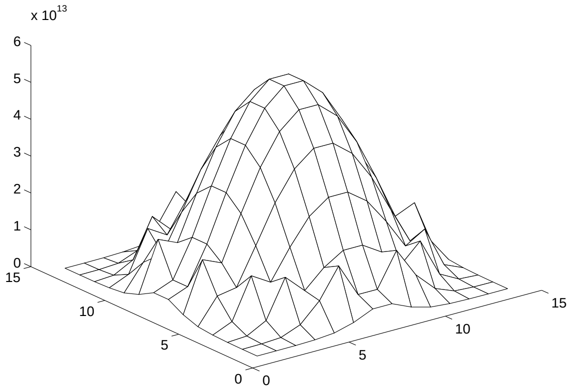

Figure 2.7: Thermal flux (averaged over cycle time) [cm^{-2} s^{-1}]

The xenon and samarium concentrations can be described by a system of linear differential equations [1]. Because the poison density converges very rapidly to its equilibrium value, the time derivatives can be set equal to zero.

$$\frac{\partial}{\partial t}\begin{bmatrix} N_{\mathrm{Xe}} \\ N_{\mathrm{Sm}} \end{bmatrix} = \begin{bmatrix} -\lambda_{\mathrm{Xe}} - \sigma_{a,\mathrm{Xe}}\phi & \\ & -\sigma_{a,\mathrm{Sm}}\phi \end{bmatrix} \cdot \begin{bmatrix} N_{\mathrm{Xe}} \\ N_{\mathrm{Sm}} \end{bmatrix} + \begin{bmatrix} \gamma_{\mathrm{tot}}\Sigma_f\phi \\ \gamma_{\mathrm{Nd}}\Sigma_f\phi \end{bmatrix} = \begin{bmatrix} 0 \\ 0 \end{bmatrix} \tag{2.53}$$

where λ is a decay constant and γ is the fractional yield of the former nuclide per fission ($\gamma_{\mathrm{tot}} = \gamma_{\mathrm{Te}} + \gamma_{\mathrm{I}} + \gamma_{\mathrm{Xe}}$). So the quasi-static solution becomes

$$N_{\mathrm{Xe}}^{i+1}(\vec{r}) = \frac{(\gamma_{\mathrm{Te}} + \gamma_{\mathrm{I}} + \gamma_{\mathrm{Xe}})\Sigma_f^i(\vec{r})\phi^i(\vec{r})}{\lambda_{\mathrm{Xe}} + \sigma_{a,\mathrm{Xe}}\phi^i(\vec{r})}, \tag{2.54}$$

$$N_{\mathrm{Sm}}^{i+1}(\vec{r}) = \frac{\gamma_{\mathrm{Nd}}\Sigma_f^i(\vec{r})}{\sigma_{a,\mathrm{Sm}}}. \tag{2.55}$$

The influence of the reactor poisons on the cross sections will be examined in the next section.

2.6 Homogenization of the cross sections

To calculate ϕ^i we need to know the cross sections Σ^i. The concentrations we obtained from the burnup equations are now used to approximate the cross sections in the reactor. The core is divided into fuel elements and each fuel element contains a cylindrical rod of uranium and moderator (e.g. water). We assume that the cross sections in each fuel element are constant in space by taking a volume weighted average over each fuel element. So the cross sections in period T_i are related to the nuclide densities by

$$\Sigma^i = \frac{\sum_n [V_n^i \Sigma_n^i]}{\sum_n [V_n^i]}, \tag{2.56}$$

where V_n^i is the volume of the nuclides of type n in period T_i.

2.6.1 Fission cross section

By discarding the nuclides with very small volumes or with very small fission cross sections, we get the following expression

$$\Sigma_f^i = \frac{V_5^i \Sigma_{f5}^i + V_8^i \Sigma_{f8}^i + V_9^i \Sigma_{f9}^i}{V_{\text{tot}}}, \tag{2.57}$$

where indices 5, 8 and 9 denote ${}^{235}_{92}\text{U}$, ${}^{238}_{92}\text{U}$ and ${}^{239}_{94}\text{Pu}$ respectively.
We know that V_n^i is related to the number of nuclide atoms $\mathcal{N}_n^i$ by

$$\frac{\mathcal{N}_n^i}{V_n^i} = \frac{\rho_n}{A_n} N_A = N_n^i, \tag{2.58}$$

with N_A the constant of Avogadro, A_n the mass of a nuclide of kind n relative to a neutron mass and ρ_n the mass density of a nuclide of type n. Substitution yields

$$\Sigma_f^i = \frac{\frac{\mathcal{N}_5^i}{N_5^i} \Sigma_{f5}^i + \frac{\mathcal{N}_8^i}{N_8^i} \Sigma_{f8}^i + \frac{\mathcal{N}_9^i}{N_9^i} \Sigma_{f9}^i}{V_{\text{tot}}}. \tag{2.59}$$

This expression can be written as

$$\begin{aligned} \Sigma_f^i &= \begin{bmatrix} \frac{\Sigma_{f5}^i}{N_5^i} & \frac{\Sigma_{f8}^i}{N_8^i} & \frac{\Sigma_{f9}^i}{N_9^i} \end{bmatrix} \cdot \begin{bmatrix} \mathcal{N}_5^i / V_{\text{tot}} \\ \mathcal{N}_8^i / V_{\text{tot}} \\ \mathcal{N}_9^i / V_{\text{tot}} \end{bmatrix} \\ &= \begin{bmatrix} \sigma_{f5} & \sigma_{f8} & \sigma_{f9} \end{bmatrix} \cdot \vec{N}^i \\ &= \vec{\sigma}_f \cdot \vec{N}^i. \end{aligned} \tag{2.60}$$

2.6.2 Absorption cross section

Because of the presence of the reactor poisons ${}^{135}_{54}\text{Xe}$ and ${}^{149}_{62}\text{Sm}$ (see section 2.5.2) the absorption cross section depends on the fissionable nuclide density but also on the poison density. So we introduce a poison density vector and a poison cross section vector

$$\vec{N}_p^i(\vec{r}) = \begin{bmatrix} N_{\text{Xe}}^i(\vec{r}) \\ N_{\text{Sm}}^i(\vec{r}) \end{bmatrix}, \qquad \vec{\sigma}_{a,p} = \begin{bmatrix} \sigma_{a,\text{Xe}} & \sigma_{a,\text{Sm}} \end{bmatrix}. \tag{2.61}$$

And the absorption cross section can be written as

$$\Sigma_a^i = \vec{\sigma}_a \cdot \vec{N}^i + \vec{\sigma}_{a,p} \cdot \vec{N}_p^i. \tag{2.62}$$

2.6.3 Scattering cross section

The moderator, e.g. water (H_2O) or heavy water (D_2O), is especially chosen for reducing the energy of neutrons by scattering. So the global scattering cross section depends on the scattering cross sections of the nuclides and of the moderator:

$$\Sigma_s^i = \vec{\sigma}_s \cdot \vec{N}^i + \frac{V_{\text{mod}}}{V_{\text{tot}}} \Sigma_{s,\text{mod}}. \tag{2.63}$$

2.6.4 Transport cross section

The transport cross section is

$$\Sigma_{tr,n} = \Sigma_{a,n} + (1 - \overline{\mu}_0)\Sigma_{s,n}, \tag{2.64}$$

with $\overline{\mu}_0$ the average value of the cosine of the scattering angle in an isotropic system. For heavy nuclides the value of $1 - \overline{\mu}_0$ is almost 1. So for the transport cross section approximation we use

$$\Sigma_{tr}^i = (\vec{\sigma}_a + \vec{\sigma}_s) \cdot \vec{N}^i + \vec{\sigma}_{a,p} \cdot \vec{N}_p^i + \left(1 - \overline{\mu}_{0,\mathrm{mod}}\right) \frac{V_{\mathrm{mod}}}{V_{\mathrm{tot}}} \Sigma_{s,\mathrm{mod}}. \tag{2.65}$$

2.7 Summary of the forward calculations

At the Begin Of Cycle (BOC) we know the density vector $\vec{N}^i$, with $i = 0$, for each fuel element. Now the cross sections in each fuel element can be approximated by

$$\Sigma_f^i = \vec{\sigma}_f \cdot \vec{N}^i \tag{2.66}$$

$$\Sigma_a^i = \vec{\sigma}_a \cdot \vec{N}^i + \vec{\sigma}_{a,p} \cdot \vec{N}_p^i \tag{2.67}$$

$$\Sigma_{tr}^i = \vec{\sigma}_t \cdot \vec{N}^i + \vec{\sigma}_{a,p} \cdot \vec{N}_p^i + \left(1 - \overline{\mu}_{0,\mathrm{mod}}\right) \frac{V_{\mathrm{mod}}}{V_{\mathrm{tot}}} \Sigma_{s,\mathrm{mod}} \tag{2.68}$$

These cross sections can be substituted into the stationary neutron transport equation with eigenvalue (k, α or r) or in one of its approximations, for example the diffusion equation with eigenvalue k:

$$\nabla \cdot \frac{1}{3\Sigma_{tr}^i(\vec{r})} \nabla \phi^i(\vec{r}) + \left(\frac{\nu}{k^i} \Sigma_f^i(\vec{r}) - \Sigma_a^i(\vec{r}) \right) \phi^i(\vec{r}) = 0, \tag{2.69}$$

with the boundary condition that there is no inward neutron flow through the boundary surface of the core:

$$\phi^i(\vec{r}) + \frac{2}{3\Sigma_{tr}^i(\vec{r})} \vec{n} \cdot \nabla \phi^i(\vec{r}) = 0. \tag{2.70}$$

First calculate the eigenvalue k^i, α^i or r^i with an algorithm analogous to the one described in section 2.3.1. Then, with this eigenvalue, solve eq. 2.69 with boundary condition 2.70 and normalize the flux to the desired power level P.

Now we can use the burnup equations to compute the nuclide densities and the poison densities at a following time step by the equations 2.49, 2.54 and 2.55, which have the form:

$$\vec{N}^{i+1}(\vec{r}) = \mathbf{B}(\vec{r}) \vec{N}^i(\vec{r}) + \vec{C}(\vec{r}) \tag{2.71}$$

Now let $i := i + 1$ and the algorithm can be processed again until the system becomes subcritical, so when $k^i < 1$.

All the steps described before are summarized in the following program:

```
N⃗⁰(r⃗) is given
i := −1
Begin repeat
   i := i + 1
   Calculate Σⁱ(r⃗) for each fuel element
   Calculate kⁱ
   Solve the diffusion equation for φⁱ(r⃗)
   Normalize φⁱ(r⃗) at the desired power level P
   Calculate N⃗ⁱ⁺¹(r⃗) for each fuel element
Repeat until kⁱ < 1
Refuel the reactor core
```

Chapter 3

Numerically solving the diffusion equation

In this chapter we focus particularly on the 2-dimensional diffusion equation with eigenvalue k:

$$\nabla \cdot \frac{1}{3\Sigma_{tr}(\vec{r})} \nabla \phi(\vec{r}) + \left(\frac{\nu}{k} \Sigma_f(\vec{r}) - \Sigma_a(\vec{r}) \right) \phi(\vec{r}) = 0, \tag{3.1}$$

with boundary condition

$$\phi(\vec{r}) + \frac{2}{3\Sigma_{tr}(\vec{r})} \frac{\partial}{\partial n} \phi(\vec{r}) = 0. \tag{3.2}$$

3.1 Difference equations

In this section we describe one particular finite difference scheme. Consider a square core with $n \times n$ fuel elements with length h cm, l cm apart. We apply the method of finite differences on the 2-dimensional diffusion equation. The core is divided into fuel elements and the flux in the fuel element with position (i, j) is $\phi(i, j)$. (See figure 3.1)

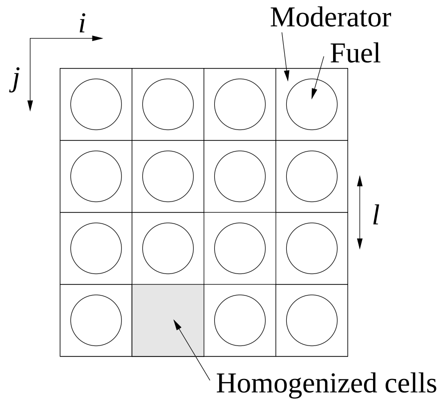

Figure 3.1: A square core

Each differentiation is replaced by a central difference quotient:

$$\frac{\partial \phi}{\partial x}(x, y) = \frac{\phi(i + \frac{1}{2}, j) - \phi(i - \frac{1}{2}, j)}{l} \tag{3.3}$$

Derivatives in respect to y are treated similar. Diffusion equation 3.1 then becomes a system of n^2 equations

$$\begin{aligned}
0 &= \frac{1}{\Sigma_{tr}(i+\frac{1}{2},j)}\phi(i+1,j) + \frac{1}{\Sigma_{tr}(i,j+\frac{1}{2})}\phi(i,j+1) \\
&- \left(\frac{1}{\Sigma_{tr}(i+\frac{1}{2},j)} + \frac{1}{\Sigma_{tr}(i,j+\frac{1}{2})} + \frac{1}{\Sigma_{tr}(i-\frac{1}{2},j)} + \frac{1}{\Sigma_{tr}(i,j-\frac{1}{2})}\right)\phi(i,j) \\
&+ 3l^2\left(\frac{\nu}{k}\Sigma_f(i,j) - \Sigma_a(i,j)\right)\phi(i,j) \\
&+ \frac{1}{\Sigma_{tr}(i-\frac{1}{2},j)}\phi(i-1,j) + \frac{1}{\Sigma_{tr}(i,j-\frac{1}{2})}\phi(i,j-1),
\end{aligned} \tag{3.4}$$

where $i = 1,\ldots,n$ and $j = 1,\ldots,n$. The cross sections halfway two grid points are approximated by

$$\begin{aligned}
\Sigma_{tr}(i+\frac{1}{2},j) &= \frac{\Sigma_{tr}(i+1,j)+\Sigma_{tr}(i,j)}{2}, \\
\Sigma_{tr}(i-\frac{1}{2},j) &= \frac{\Sigma_{tr}(i-1,j)+\Sigma_{tr}(i,j)}{2}, \\
\Sigma_{tr}(i,j+\frac{1}{2}) &= \frac{\Sigma_{tr}(i,j+1)+\Sigma_{tr}(i,j)}{2}, \\
\Sigma_{tr}(i,j-\frac{1}{2}) &= \frac{\Sigma_{tr}(i,j-1)+\Sigma_{tr}(i,j)}{2}.
\end{aligned} \tag{3.5}$$

When the fluxes halfway two grid points are treated as averages of their neighbour points, the boundary condition yields the following expressions

$$\begin{aligned}
\phi(n+1,j) &= \frac{8-3l[\Sigma_{tr}(n,j)+\Sigma_{tr}(n+1,j)]}{8+3l[\Sigma_{tr}(n,j)+\Sigma_{tr}(n+1,j)]}\phi(n,j), \\
\phi(i,n+1) &= \frac{8-3l[\Sigma_{tr}(i,n)+\Sigma_{tr}(i,n+1)]}{8+3l[\Sigma_{tr}(i,n)+\Sigma_{tr}(i,n+1)]}\phi(i,n), \\
\phi(0,j) &= \frac{8-3l[\Sigma_{tr}(1,j)+\Sigma_{tr}(0,j)]}{8+3l[\Sigma_{tr}(1,j)+\Sigma_{tr}(0,j)]}\phi(1,j), \\
\phi(i,0) &= \frac{8-3l[\Sigma_{tr}(i,1)+\Sigma_{tr}(i,0)]}{8+3l[\Sigma_{tr}(i,1)+\Sigma_{tr}(i,0)]}\phi(i,1).
\end{aligned} \tag{3.6}$$

When the $\phi(i,j)$, $i,j = 0,\ldots,n+1$, are placed in a vector $\mathbf{x}$, with eqs. 3.4 and 3.6 we get a matrix equation

$$\mathbf{A}\vec{\phi} = \vec{0}. \tag{3.7}$$

And k follows from

$$\det(\mathbf{A}) = 0. \tag{3.8}$$

This finite difference method (FEM) will later be used in the fast forward algorithm (FFA).

3.1.1 Example for only one fuel element

When we use only one fuel element and also assume that the element is embedded in surroundings with the same cross sections

$$
\begin{aligned}
\Sigma_{tr}(n+1,j) &= \Sigma_{tr}(n,j), \\
\Sigma_{tr}(0,j) &= \Sigma_{tr}(1,j), \\
\Sigma_{tr}(i,n+1) &= \Sigma_{tr}(i,n), \\
\Sigma_{tr}(i,0) &= \Sigma_{tr}(i,1),
\end{aligned}
$$

the difference equation 3.4 reduces to

$$
\left(\frac{2}{4+3l\Sigma_{tr}(1,1)} - \frac{l}{4}\left(\frac{\nu}{k}\Sigma_f(1,1) - \Sigma_a(1,1)\right)\right)\phi(1,1) = 0. \tag{3.9}
$$

The flux ϕ is not determined by this equation, but follows from the desired power level and the eigenvalue k can be solved.

$$
\phi = \frac{P}{\mu_f h l^2 \Sigma_f}, \tag{3.10}
$$

$$
k = \frac{\nu\Sigma_f}{8\left[4l+3l^2\Sigma_{tr}\right]^{-1} + \Sigma_a}. \tag{3.11}
$$

In figure 3.2 the multiplication factor k is plotted as function of the width l. (Parameters used: $\nu = 2.6$, $\sigma_f = 1.29$b, $\sigma_{tr} = 6.8$b, $\sigma_a = 1.50$b)

This figure shows that k converges to

$$
k_\infty = \lim_{l\to\infty} = \frac{\nu\Sigma_f}{\Sigma_a}, \tag{3.12}
$$

with k_∞ the multiplication factor of an infinite, so non-leaking, reactor. With the parameters used in the figure we get $k_\infty = 2.32$. The criticality condition $k = 1$ yields

$$
l_{\text{crit}} = \frac{2}{3\Sigma_{tr}}\left(\sqrt{1+\frac{6\Sigma_{tr}}{\nu\Sigma_f - \Sigma_a}} - 1\right). \tag{3.13}
$$

(So $l_{\text{crit}} = 7.86$cm in our case.) Figure 3.3 shows l_{crit} as function of Σ_a. There is a vertical asymptote at $\Sigma_a = \nu\Sigma_f$, which means that it is impossible to keep a reactor critical if the production rate of neutrons is less than the absorption rate.

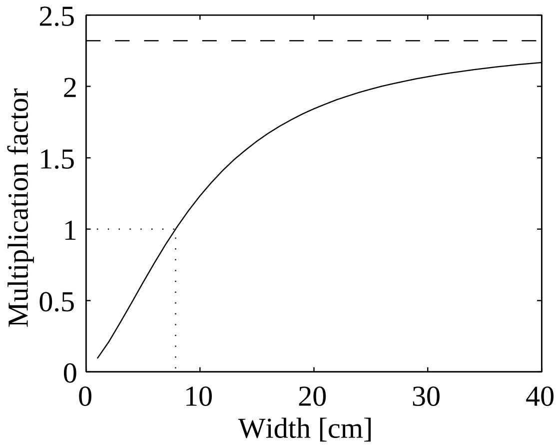

Figure 3.2: The multiplication factor k as function of width l

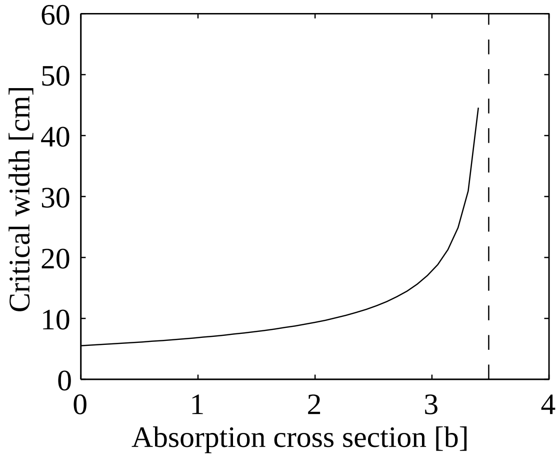

Figure 3.3: The critical width l_{crit} as function of the absorption cross section Σ_a

Chapter 4

The adjoint equation

In this section the adjoint equation is used in developing a fast forward algorithm. With this algorithm reloading patterns that are variations of one starting pattern can be quickly evaluated and the optimal pattern can be found.

Let $\mathbf{T}$ be an operator on a function ϕ. Function ϕ has to satisfy certain boundary conditions. The adjoint operator $\mathbf{T}^*$ will operate on a function ψ^*, called the adjoint function, which may satisfy boundary conditions different from those satisfied by ϕ. $\mathbf{T}^*$ is related to $\mathbf{T}$ by the following innes products:

$$(\psi^*, \mathbf{T}\phi) = (\phi, \mathbf{T}^*\psi^*). \tag{4.1}$$

We will use the following definition for the inner product of two functions

$$(\psi, \phi) = \int_V \int_0^\infty \int_{4\pi} \psi(\vec{r}, E, \vec{\Omega}) \phi(\vec{r}, E, \vec{\Omega}) \, dV \, dE \, d\Omega. \tag{4.2}$$

An operator $\mathbf{T}$ is called self-adjoint if it satisfies

$$(\psi, \mathbf{T}\phi) = (\phi, \mathbf{T}\psi). \tag{4.3}$$

We now will apply this theory to the neutron transport equation 2.7.

4.1 The adjoint transport operator

We consider the time independent form of the neutron transport equation and define the transport operator $\mathbf{T}$ as

$$\begin{aligned} \mathbf{T}\Phi(\vec{r}, E, \vec{\Omega}) &= \frac{\chi(E)}{4\pi} \int_0^\infty \int_{4\pi} \nu(E') \Sigma_f(\vec{r}, E') \Phi(\vec{r}, E', \vec{\Omega}') \, dE' \, d\Omega' \\ &+ \int_0^\infty \int_{4\pi} \Sigma_s(\vec{r}, E' \to E, \vec{\Omega}' \to \vec{\Omega}) \Phi(\vec{r}, E', \vec{\Omega}') \, dE' \, d\Omega' \\ &- \vec{\Omega} \cdot \nabla \Phi(\vec{r}, E, \vec{\Omega}) \\ &- \Sigma_t(\vec{r}, E) \Phi(\vec{r}, E, \vec{\Omega}). \end{aligned} \tag{4.4}$$

If we apply relation 4.1 we can derive $\mathbf{T}^*$ and the boundary condition on the adjoint Φ^* [1]:

$$\begin{aligned}
\mathbf{T}^*\Phi^*(\vec{r},E,\vec{\Omega}) &= \frac{1}{4\pi}\nu(E)\Sigma_f(\vec{r},E)\int_0^\infty\int_{4\pi}\chi(E')\Phi^*(\vec{r},E',\vec{\Omega}')\,dE'\,d\Omega' \\
&+ \int_0^\infty\int_{4\pi}\Sigma_s(\vec{r},E\to E',\vec{\Omega}\to\vec{\Omega}')\Phi^*(\vec{r},E',\vec{\Omega}')\,dE'\,d\Omega' \\
&+ \vec{\Omega}\cdot\nabla\Phi^*(\vec{r},E,\vec{\Omega}) \\
&- \Sigma_t(\vec{r},E)\Phi^*(\vec{r},E,\vec{\Omega}).
\end{aligned} \tag{4.5}$$

The transport equation and the adjoint transport equation are thus:

$$\mathbf{T}\Phi(\vec{r},E,\vec{\Omega}) = -Q(\vec{r},E,\vec{\Omega}) \quad \text{with} \quad \Phi(\vec{r}_b,E,\vec{\Omega}) = 0 \text{ for } \vec{n}\cdot\vec{\Omega} < 0, \tag{4.6}$$

$$\mathbf{T}^*\Phi^*(\vec{r},E,\vec{\Omega}) = -Q^*(\vec{r},E,\vec{\Omega}) \quad \text{with} \quad \Phi^*(\vec{r}_b,E,\vec{\Omega}) = 0 \text{ for } \vec{n}\cdot\vec{\Omega} > 0. \tag{4.7}$$

In eq. 4.6 an extra neutron source Q is introduced, which of course depends on the modelled physical situation. In the adjoint equation 4.7 an adjoint source Q^* has been introduced. The choice of Q^* is free.

Note that the transport equation is not self-adjoint. To show that the inner products are not equal, compare the flow terms $(\Phi^*, -\vec{\Omega}\cdot\nabla\Phi)$ and $(\Phi, -\vec{\Omega}\cdot\nabla\Phi^*)$. In general, these two quantities are different. Similarly, the scatter terms are different. Hence, it follows that $(\Phi^*, \mathbf{T}\Phi) \neq (\Phi, \mathbf{T}\Phi^*)$ and the transport operator is not self-adjoint.

4.1.1 The adjoint of the $1\frac{1}{2}$-group diffusion operator

The $1\frac{1}{2}$-group diffusion theory was derived from the 2-group diffusion theory by neglecting the thermal neutron diffusion term. (See section 2.4.2) The $1\frac{1}{2}$-group diffusion equation can be written as

$$\begin{bmatrix} \nabla\cdot\frac{1}{3\Sigma_{tr}^1}\nabla + \nu\Sigma_f^1 - \Sigma_a^1 - \Sigma_s^{1\to2} & \nu\Sigma_f^2 \\ \Sigma_s^{1\to2} & -\Sigma_a^2 \end{bmatrix} \cdot \begin{bmatrix} \phi^1 \\ \phi^2 \end{bmatrix} = \begin{bmatrix} 0 \\ 0 \end{bmatrix} \tag{4.8}$$

The adjoint equation is

$$\begin{bmatrix} \nabla\cdot\frac{1}{3\Sigma_{tr}^1}\nabla + \nu\Sigma_f^1 - \Sigma_a^1 - \Sigma_s^{1\to2} & \Sigma_s^{1\to2} \\ \nu\Sigma_f^2 & -\Sigma_a^2 \end{bmatrix} \cdot \begin{bmatrix} \phi^{*1} \\ \phi^{*2} \end{bmatrix} = \begin{bmatrix} 0 \\ 0 \end{bmatrix} \tag{4.9}$$

Solving this system gives an equation for the fast adjoint:

$$\nabla\cdot\frac{1}{3\Sigma_{tr}^1(\vec{r})}\nabla\phi^{*1}(\vec{r}) + \left(\nu\Sigma_f^1(\vec{r}) + \nu\Sigma_f^2(\vec{r})\frac{\Sigma_s^{1\to2}(\vec{r})}{\Sigma_a^2(\vec{r})} - \Sigma_s^{1\to2}(\vec{r}) - \Sigma_a^1(\vec{r})\right)\phi^{*1} = 0 \tag{4.10}$$

and one for the thermal adjoint:

$$\phi^{*2}(\vec{r}) = \frac{\nu\Sigma_f^2(\vec{r})}{\Sigma_a^2(\vec{r})}\phi^{*1}(\vec{r}) \tag{4.11}$$

So by reducing the order, the non-self-adjoint, second order $1\frac{1}{2}$-group diffusion operator is split into two first order operators. Comparison of eq. 4.10 with eq. 2.32 shows that the fast operator is self-adjoint and comparison of eq. 4.11 with eq. 2.31 shows that the thermal operator is not self-adjoint.

4.2 The functional J_{Q^*}

The interpretation of the adjoint function depends on the choice of the adjoint source. If the adjoint source is chosen to be a macroscopic cross section $Q^* = \Sigma$ [cm^{-1}], then the adjoint function Φ^* has no dimension and can be interpreted as the importance of a neutron in position $\vec{r}$ with direction $\vec{\Omega}$ and energy E. The boundary condition for the adjoint transport equation means that neutrons leaving the volume are not important. But, as we will see, other choices for the adjoint source and for the adjoint boundary condition are also possible.

We multiply eq. 4.6 by Φ^* and eq. 4.7 by Φ. Subtraction of the results and integration over all variables gives

$$(Q, \Phi^*) - (Q^*, \Phi) = 0. \tag{4.12}$$

Until now, we assumed that there are no incoming neutrons and no outgoing adjoint (eqs. 4.6, 4.7). We now postulate new boundary conditions

$$\Phi(\vec{r}_b, E, \vec{\Omega}) = \Phi_{\text{in}}(\vec{r}_b, E, \vec{\Omega}) \quad \text{for} \quad \vec{n} \cdot \vec{\Omega} < 0, \tag{4.13}$$

$$\Phi^*(\vec{r}_b, E, \vec{\Omega}) = \Phi^*_{\text{out}}(\vec{r}_b, E, \vec{\Omega}) \quad \text{for} \quad \vec{n} \cdot \vec{\Omega} > 0. \tag{4.14}$$

Analogous to the way we derived relation 4.12 we now get this relation for the case of non-zero boundary conditions:

$$(Q, \Phi^*) - (Q^*, \Phi) = \iiint_{\vec{n}\cdot\vec{\Omega}<0} \vec{n} \cdot \vec{\Omega} \left(\Phi^*\Phi_{\text{in}} - \Phi\Phi^*_{\text{out}}\right) \, dA \, dE \, d\Omega, \tag{4.15}$$

where dA is a boundary element. Now consider the linear functional J_{Q^*} of Φ:

$$J_{Q^*} = (Q^*, \Phi) \,. \tag{4.16}$$

If the function Q^* is made to represent the characteristics of a measuring instrument, then the functional J_{Q^*} gives the measurement. Some examples are listed in table 4.1.

Table 4.1: Instrument characteristics

Q^*	J_{Q^*}
$\delta(\vec{r} - \vec{r}_0)$	The neutron flux at $\vec{r} = \vec{r}_0$
Σ_a	The total number of absorption events
$-\vec{\Omega} \cdot \nabla$	A measure for the neutron flow

4.3 Perturbation theory

We want to see how small perturbations in the cross sections ($\delta\Sigma$) influence the flux. We assume that the perturbed flux ϕ' is the sum of the exact flux ϕ and a perturbation $\delta\phi$. So

$$\phi' = \phi + \delta\phi,\ D' = D + \delta D \text{ and } \Sigma' = \Sigma + \delta\Sigma. \tag{4.17}$$

The diffusion equation for the perturbed flux ϕ' and the adjoint equation are

$$\nabla D'\nabla\phi' + \Sigma'\phi' = -Q' \quad \text{with} \quad 2D'\frac{\partial\phi'}{\partial n} + \phi' = \phi'_{\text{in}}, \tag{4.18}$$

$$\nabla D\nabla\phi^* + \Sigma\phi^* = -Q^* \quad \text{with} \quad 2D\frac{\partial\phi^*}{\partial n} + \phi^* = \phi^*_{\text{out}}, \tag{4.19}$$

where $\Sigma = \nu\Sigma_f - \Sigma_a - r(\Sigma_{a,\text{B}} - \Sigma_{a,\text{mod}})$ (For brevity reasons we use the one-group model, but if you want to extend to the $1\frac{1}{2}$-group model, use the replacements mentioned in 2.33-2.36.) In the case of the one-group or $1\frac{1}{2}$-group diffusion theory we define the inner product as

$$(\psi, \phi) = \int_V \psi(\vec{r})\phi(\vec{r})\,dV. \tag{4.20}$$

Relation 4.15 becomes

$$(Q, \phi^*) - (Q^*, \phi) = \frac{1}{2}\int_{\partial V} (\phi\phi^*_{\text{out}} - \phi^*\phi_{\text{in}})\ dA. \tag{4.21}$$

We multiply the perturbed equation 4.18 with ϕ^* and the adjoint equation 4.19 with ϕ', integrate the results over volume V and subtract the two to obtain

$$\begin{aligned} \int_V (\phi^*\nabla D'\nabla\phi' - \phi'\nabla D\nabla\phi^*)\ dV \quad &+ \quad \int_V (\phi^*\Sigma'\phi' - \phi'\Sigma\phi^*)\ dV. \\ &= \quad \int_V (\phi' Q^* - \phi^* Q')\ dV. \end{aligned} \tag{4.22}$$

This expression can be simplified by partial integration of the first term, substitution of the boundary conditions (4.18, 4.19) and application of relation 4.21:

$$\begin{aligned} -\int_V \delta D\nabla\phi^*\cdot\nabla\phi'\,dV \quad &+ \quad \frac{1}{2}\int_{\partial V} (\phi^*\delta\phi_{\text{in}} - \delta\phi\phi^*_{\text{out}})\ dA \\ &+ \quad \int_V \delta\Sigma\phi^*\phi'\,dV = \int_V (\delta\phi Q^* - \phi^*\delta Q)\ dV. \end{aligned} \tag{4.23}$$

We define functional J_{Q^*} as

$$J_{Q^*} = (\phi, Q^*)\,. \tag{4.24}$$

Eq. 4.21 learns us that the value of the functional J_{Q^*} can be computed in another way:

$$J_{Q^*} = (Q, \phi^*) + \frac{1}{2}\int_{\partial V} \phi^*\phi_{\text{in}}\,dA - \frac{1}{2}\int_{\partial V} \phi\phi^*_{\text{out}}\,dA. \tag{4.25}$$

The solution of the perturbed problem is $\phi' = \phi + \delta\phi$. Perturbation $\delta\phi$ changes the value of functional J_{Q^*} with δJ_{Q^*} ($JQ^* = J_{Q^*} + \delta J_{Q^*}$), where

$$\delta J_{Q^*} = (\delta\phi, Q^*)\,. \tag{4.26}$$

And eq. 4.23 gives us a second way to calculate the variation of this functional:

$$\begin{aligned} \delta J_{Q^*} &= (\delta Q, \phi^*) + \frac{1}{2}\int_{\partial V} \phi^* \delta\phi_{\text{in}}\, dA - \frac{1}{2}\int_{\partial V} \delta\phi\phi^*_{\text{out}}\, dA \\ &- (\delta D, \nabla\phi^* \cdot \nabla\phi') + (\delta\Sigma, \phi^*\phi')\,. \end{aligned} \tag{4.27}$$

This expression shows us where changes in the variables have a significant influence on J_{Q^*}. For example, only there where $\nabla\phi^* \cdot \nabla\phi'$ is large, a small variation of the diffusion coefficient D will cause a significant variation of J_{Q^*}.

4.4 Engineering constraints

As mentioned before, different objective functions can be chosen in the optimization of a reloading pattern. For now, we choose to maximize the burnup of the discharged fuel elements and to minimize the burnup in the other elements. Thus we try to make efficient use of fuel and to reduce the amount of nuclear waste.

During the cycle time the reactor is subjected to certain engineering constraints. And under these conditions we try to maximize our objective function. In this section we formulate the engineering constraints.

1. The local power should be limited, because of possible meltdown when the temperature somewhere in the core becomes too high. So the flux in each fuel element c is subjected to

$$\int_V \phi Q^*_p\, dV + \int_{\partial V} \phi\phi^*_p\, dA \leq P_{\text{crit}}, \tag{4.28}$$

   where the characteristic functions are defined as

$$Q^*_p(x,y) = \begin{cases} \mu_f \Sigma_f(x,y) & \text{if} \quad (x,y) \in c \\ 0 & \text{if} \quad (x,y) \notin c \end{cases} \tag{4.29}$$

$$\phi^*_p(x,y) = 0 \tag{4.30}$$

2. The reactor should also operate at a constant power level P:

$$\mu_f \int_V \Sigma_f \phi\, dV = P. \tag{4.31}$$

3. The leakage of neutrons through the core boundaries slowly destructs the core mantle. So we also bound the leakage by

$$\int_V \phi Q_l^* \, dV + \int_{\partial V} \phi \phi_l^* \, dA \leq L_{\text{crit}}, \tag{4.32}$$

where the characteristic functions are defined as

$$Q_l^*(x,y) = 0 \tag{4.33}$$
$$\phi_l^*(x,y) = 1 \tag{4.34}$$

4. From practical point of view it is required that the cycle time is a fixed time. So maintenance and cleaning can be done when the reactor is down for fuel refreshment. So for example

$$nT = 1 \text{ year} \tag{4.35}$$

4.5 Possible objective functions

To optimize the reloading pattern we link a unique quantity to each reloading pattern. This link is called the objective function. We say that the optimal pattern is the one with the highest possible objective function. In this section we examine different objective functions.

I: Maximizing the burnup in the oldest fuel elements
Define $B_5(c)$ as the burnup of the ${}^{235}_{92}\text{U}$ in a fuel element c:

$$B_5(c) = \begin{bmatrix} 1 & 0 & 0 \end{bmatrix} \cdot \left(\vec{N}^0(c) - \vec{N}^n(c) \right) \tag{4.36}$$

With the burnup equations this can be written as

$$B_5(c) = \left(1 - \exp\left(-\sigma_{a5} \sum_{j=0}^{n-1} \phi^j(c) T \right) \right) N_5^0(c) \tag{4.37}$$

We now want to maximize the relative burnup of the ${}^{235}_{92}\text{U}$ in the oldest fuel batch F_{old} over all possible initial nuclide densities $N_5^0(c)$. So

$$\max_{N_5^0(c)} \frac{\sum_{c \in F_{\text{old}}} \left(1 - \exp\left(-\sigma_{a5} \sum_{j=0}^{n-1} \phi^j(c) T \right) \right) N_5^0(c)}{\sum_{c \in F_{\text{old}}} N_5^0(c)} \tag{4.38}$$

If we have to maximize over all possible permutations of one available $N_5(c)$ then

$$\min_{N_5^0(c) \in P(N_5(c))} \sum_{c \in F_{\text{old}}} \exp\left(-\sigma_{a5} \sum_{j=0}^{n-1} \phi^j(c) T \right) N_5^0(c) \tag{4.39}$$

And this is equal to

$$\min_{\vec{N}^0(c)\in P(\vec{N}(c))} \sum_{c\in F_{\text{old}}} \begin{bmatrix} 1 & 0 & 0 \end{bmatrix} \cdot \vec{N}^n(c) \tag{4.40}$$

So we see that, if $\vec{N}^0(c)$ has to be a permutation of a given $\vec{N}(c)$, maximizing the burnup or the relative burnup is equal to minimizing the EOC nuclide density N_5^n.

II: Maximizing the burnup in the oldest fuel elements and minimizing the burnup in the younger fuel elements
Another possibility is to minimize the burnup in the newer fuel bundles and at the same time to maximize the burnup in the oldest fuel bundles. Then we get the following objective function:

$$\max_{\vec{N}^0(c)\in P(\vec{N}(c))} \begin{bmatrix} 1 & 0 & 0 \end{bmatrix} \cdot \left(\sum_{c\notin F_{\text{old}}} \vec{N}^n(c) - \sum_{c\in F_{\text{old}}} \vec{N}^n(c) \right) \tag{4.41}$$

III: A linear combination of I+II
Because the number of oldest fuel elements is $n_{\text{age}} - 1$ times smaller than the number of other fuel elements, the following objective function can be used:

$$\max_{\vec{N}^0(c)\in P(\vec{N}(c))} \begin{bmatrix} 1 & 0 & 0 \end{bmatrix} \cdot \left(\sum_{c\notin F_{\text{old}}} \vec{N}^n(c) - (n_{\text{age}} - 1) \sum_{c\in F_{\text{old}}} \vec{N}^n(c) \right), \tag{4.42}$$

where n_{age} is the number of age groups.

IV: Maximizing the boric acid concentration at EOC
We can also try to maximize the reactivity of the core at end of cycle. This is equal to maximizing r^n:

$$\max_{\vec{N}^0(c)\in P(\vec{N}(c))} r^n. \tag{4.43}$$

4.6 Perturbed cross sections

A forward algorithm for calculation of the flux distribution over the core was presented in section 2.7 (Strategy). The burnup of the fuel causes a variation in the cross sections, and consequently in the flux. In this section we want to examine the influence of variations in the cross sections on the neutron flux.

We assume that the influence of the perturbation of the neutron flux ($\delta\phi$) on the right hand side of eq. 4.27 is small and that the variation δJ_{Q^*} of the functional J_{Q^*} is only caused by the variation $\delta\Sigma$ of the cross section Σ. So eq. 4.27 reduces to

$$\delta J_{Q^*} = (\delta\Sigma, \phi^*\phi). \tag{4.44}$$

At time $t = iT$ the cross sections are discontinuous and we define the variation $\delta\Sigma^i = \Sigma^{i+1} - \Sigma^i$. Now the variations in the cross section Σ are variations in the fission and absorption cross sections:

$$\begin{aligned} \Sigma_f^i &\longrightarrow \Sigma_f^{i+1} \\ \Sigma_a^i &\longrightarrow \Sigma_a^{i+1} \end{aligned}$$

Variations in the cross sections can be divided in two kinds:

1. The uncontrolled variations, due to variations in the concentrations of fissionable nuclides and poison

2. The controlled variations, due to control rod movements or variations in the concentration of boric acid (=variations in the eigenvalue r).

So we can describe $\delta\Sigma = \delta\Sigma_f + \delta\Sigma_a$ with

$$\begin{aligned} \delta\Sigma_f^i &= \vec{\sigma}_f \cdot \delta\vec{N} = \vec{\sigma}_f \cdot (\vec{N}^{i+1} - \vec{N}^i), && (4.45) \\ \delta\Sigma_a^i &= \vec{\sigma}_a \cdot \delta\vec{N} + \vec{\sigma}_{a,p} \cdot \delta\vec{N}_p + \delta r^i(\Sigma_{a,\mathrm{B}} - \Sigma_{a,\mathrm{mod}}) \\ &= \vec{\sigma}_a \cdot (\vec{N}^{i+1} - \vec{N}^i) + \vec{\sigma}_{a,p} \cdot (\vec{N}_p^{i+1} - \vec{N}_p^i) + \delta r^i(\Sigma_{a,\mathrm{B}} - \Sigma_{a,\mathrm{mod}}), && (4.46) \end{aligned}$$

where $\delta r^i(\Sigma_{a,\mathrm{B}} - \Sigma_{a,\mathrm{mod}})$ is the only controlled variation.

We now assume that the perturbation of the poison density is small ($\vec{N}_p^{i+1} \approx \vec{N}_p^i$). Then δJ_{Q^*} (eq. 4.44 can be expressed by

$$\delta J_{Q^*} = \left((\nu\vec{\sigma}_f - \vec{\sigma}_a) \cdot (\vec{N}^{i+1} - \vec{N}^i)\phi^i, \phi^*\right) - \delta r^i \left((\Sigma_{a,\mathrm{B}} - \Sigma_{a,\mathrm{mod}})\phi^i, \phi^*\right). \qquad (4.47)$$

The variation of the nuclide density $(\vec{N}^{i+1} - \vec{N}^i)$ in this expression is given by the burnup equations (eqs. 2.49) and application of these equations gives

$$\begin{aligned} \delta J_{Q^*} &= -\left((\nu\vec{\sigma}_f - \vec{\sigma}_a) \cdot \left(\mathbf{I} - \exp(\mathbf{B}(\phi^i)T)\right) \vec{N}^i\phi^i, \phi^*\right) \\ &- \delta r^i \left((\Sigma_{a,\mathrm{B}} - \Sigma_{a,\mathrm{mod}})\phi^i, \phi^*\right). && (4.48) \end{aligned}$$

We choose the adjoint source to be a spatial block function. For each particular fuel element c we define a Q_c^*:

$$Q_c^*(x, y) = \begin{cases} 1 & \text{if} \quad (x, y) \in c \\ 0 & \text{if} \quad (x, y) \notin c \end{cases} \qquad (4.49)$$

The adjoint function ϕ_c^* is the solution of the adjoint equation 4.19 with adjoint source Q_c^*. Note that for every fuel element c there is a different adjoint function. In our modelled physical situation there is no neutron source and no neutron flow through the surface of the reactor. So $Q = 0$ and $\phi_{\mathrm{in}} = 0$. Now, because eq. 4.24 and eq. 4.25 are equal, we can compute $\phi_{\mathrm{out},c}^*$. We choose $\phi_{\mathrm{out},c}^*$ constant over the core boundary ∂V, so

$$\phi_{\mathrm{out},c}^* = \frac{-2\int_c \phi^i \, dV}{\int_{\partial V} \phi^i \, dA}. \qquad (4.50)$$

So with the given Q_c^* (eq. 4.49) the adjoint function ϕ_c^* is subjected to the boundary condition

$$2D\frac{\partial \phi_c^*}{\partial n} + \phi_c^* = \frac{-2\int_c \phi^i \, dV}{\int_{\partial V} \phi^i \, dA}. \tag{4.51}$$

Brief summary of sources and boundary functions

$$\begin{array}{ll} Q(x,y) = 0, & \phi_{\text{in}} = 0, \\ Q_c^*(x,y) = \left\{ \begin{array}{lll} 1 & \text{if} & (x,y) \in c \\ 0 & \text{if} & (x,y) \notin c \end{array} \right. , & \phi^*_{\text{out},c} = \frac{-2\int_c \phi^i \, dV}{\int_{\partial V} \phi^i \, dA}. \end{array} \tag{4.52}$$

Forward flux calculcation
Substitution of eq. 4.49 into the left hand side eq. 4.48 yields (see eq. 4.26)

$$\begin{aligned} \int_c \delta\phi^i \, dV &= -\left((\nu\vec{\sigma}_f - \vec{\sigma}_a) \cdot \left(\mathbf{I} - \exp(\mathbf{B}(\phi^i)T) \right) \vec{N}^i \phi^i, \phi_c^* \right) \\ &- \delta r^i \left((\Sigma_{a,\text{B}} - \Sigma_{a,\text{mod}})\phi^i, \phi_c^* \right). \end{aligned} \tag{4.53}$$

With $\phi^{i+1} = \phi^i + \delta\phi^i$, it follows that

$$\begin{aligned} \int_c \phi^{i+1} \, dV &= \int_c \phi^i \, dV - \delta r^i \left((\Sigma_{a,\text{B}} - \Sigma_{a,\text{mod}})\phi^i, \phi_c^* \right) \\ &- \left((\nu\vec{\sigma}_f - \vec{\sigma}_a) \cdot \left(\mathbf{I} - \exp(\mathbf{B}(\phi^i)T) \right) \vec{N}^i \phi^i, \phi_c^* \right). \end{aligned} \tag{4.54}$$

One can quickly calculate ϕ^{i+1} in cell c using ϕ_c^* and eq. 4.54 . To emphasize that ϕ^{i+1} is completely determined by $\phi^0, \ldots, \phi^i$ we also express the nuclide density $\vec{N}^i$ in terms of $\phi^0, \ldots, \phi^{i-1}$, using eq. 2.49:

$$\vec{N}^i = \exp\left(\mathbf{B} \left(\sum_{j=0}^{i-1} \phi^j \right) T \right) \vec{N}^0. \tag{4.55}$$

Perturbation of r
The variation in the eigenvalue r caused by the burnup can also be calculated using perturbation theory. When we choose $Q_c^* = 0$ it follows that the adjoint is equal to the neutron flux density ($\phi^* = \phi$). Using the same techniques as before we get $(\phi^i, \Sigma^i \phi^i) = 0$ and it follows that

$$\delta r^i = \frac{\left(\phi^i, (\nu\vec{\sigma}_f - \vec{\sigma}_a) \cdot (\mathbf{I} - \exp(\mathbf{B}(\phi^i)T))\, \vec{N}^i \phi^i\right)}{(\Sigma_{a,\text{B}} - \Sigma_{a,\text{mod}})(\phi^i, \phi^i)}. \tag{4.56}$$

Flux averaging
We define the average value of the neutron flux density $\bar{\phi}$ over each fuel element c by

$$\bar{\phi} = \frac{1}{V_c} \int_c \phi \, dV \tag{4.57}$$

Chapter 5

Algorithms

In this chapter the information gathered in section 4.6 is presented as an algorithm. First a fast forward algorithm is developed for use in the optimization problem. Then a backward algorithm is developed, which can be of use in future optimization methods.

5.1 List of assumptions

The algorithms described in the sections 5.2 and 5.3 are developed under certain assumptions. The essential assumptions are:

1. The perturbation of the flux density ϕ during each time step is small.
2. The cross sections and nuclide densities are homogenized over each fuel element.

And the non-essential assumptions, which can be extended or discarded in future, are:

1. The $1\frac{1}{2}$-group diffusion approximation is used.
2. The poison density $\vec{N}_p$ is constant.
3. The perturbation of the flux density ϕ is only caused by perturbations of the fission an absorption cross sections, and not by perturbations of diffusion coefficient.

5.2 Forward flux calculations

We now develop an approximate, but fast forward algorithm for the whole reactor cycle, with the initial nuclide density vector $\vec{N}^0$ as the only input parameter.

$\mathcal{F}1$. The initial ($i = 0$) nuclide density vector $\vec{N}^0$ is given. The initial cross sections are calculated with the equations of section 2.6. Now perform an eigenvalue calculation to obtain r^0, the relative volume of the boric acid in the fuel element. (Section 2.3.3) Then, the initial flux distribution ϕ^0 is found by solving the $1\frac{1}{2}$-group diffusion equation:

$$\nabla D^0 \nabla \phi^0 + \Sigma^0 \phi^0 = 0,$$

where
$$D^0 = \frac{1}{3\Sigma^0_{tr}} \text{ and } \Sigma^0 = \nu\Sigma^0_f - \Sigma^0_a - r^0(\Sigma_{a,\mathrm{B}} - \Sigma_{a,\mathrm{mod}}).$$

$\mathcal{F}2$. For each fuel element c compute the adjoint ϕ^*_c described by
$$\nabla D^0 \nabla \phi^*_c + \Sigma^0 \phi^*_c = \begin{cases} -1 & \text{if} \quad (x,y) \in c \\ 0 & \text{if} \quad (x,y) \notin c \end{cases},$$
with boundary condition
$$2D^0 \frac{\partial \phi^*_c}{\partial n} + \phi^*_c = \frac{-2\int_c \phi^0 \, dV}{\int_{\partial V} \phi^0 \, dA}.$$

$\mathcal{F}3$. If $\bar{\phi}^i$ is a solution of the diffusion equation then $\eta\bar{\phi}^i$ is also a solution, so normalize the flux density $\bar{\phi}^i$ at the desired power level P (see eq. 2.9)
$$\eta = \frac{P}{\mu_f V_c \sum_c \vec{\sigma}_f \cdot \vec{N}^i(c)\bar{\phi}^i(c)}.$$

$\mathcal{F}4$. Calculate the nuclide density vector in period T_{i+1} ($\vec{N}^{i+1}$) and two quantities necessary to evaluate eq. 4.54: $\bar{\phi}^i_{\mathrm{ctrl}}$, the flux caused by a unit variation ($\delta r = 1$) in the boric acid concentration and $\delta\bar{\phi}^i_{\mathrm{burn}}$, the flux variation caused by the burnup:
$$\begin{aligned} \vec{N}^{i+1}(c) &= \exp\left(\mathbf{B}\left(\bar{\phi}^i(c)\right)T\right)\vec{N}^i(c), \\ \bar{\phi}^i_{\mathrm{ctrl}}(c) &= \sum_{c'} (\Sigma_{a,\mathrm{B}} - \Sigma_{a,\mathrm{mod}})\bar{\phi}^i(c')\phi^*_c(c'), \\ \delta\bar{\phi}^i_{\mathrm{burn}}(c) &= \sum_{c'} (\nu\vec{\sigma}_f - \vec{\sigma}_a) \cdot \left(\vec{N}^i(c') - \vec{N}^{i+1}(c')\right)\bar{\phi}^i(c')\phi^*_c(c'). \end{aligned}$$

$\mathcal{F}5$. Calculate the variation in the eigenvalue r as in eq. 4.56
$$\delta r^i = \frac{\sum_c \left[(\nu\vec{\sigma}_f - \vec{\sigma}_a) \cdot \left(\vec{N}^{i+1}(c) - \vec{N}^i(c)\right)\bar{\phi}^i(c)^2\right]}{\sum_c \left[(\Sigma_{a,\mathrm{B}} - \Sigma_{a,\mathrm{mod}})\bar{\phi}^i(c)^2\right]}.$$

$\mathcal{F}6$. Compute the average flux density $\bar{\phi}^{i+1}$ in each fuel element c from the average flux densities in the former periods $\left(\bar{\phi}^0, \ldots, \bar{\phi}^i\right)$ with eq. 4.54
$$\bar{\phi}^{i+1}(c) \quad = \quad \bar{\phi}^i(c) - \delta r^i \bar{\phi}^i_{\mathrm{ctrl}}(c) - \delta\bar{\phi}^i_{\mathrm{burn}}(c).$$

$\mathcal{F}7$. Let $i := i + 1$ and go to step $\mathcal{F}3$.

Note that the flux in period T_{i+1} only depends on

1. the flux in period T_i
2. the controlled variations in the cross sections
3. the variations in the cross sections caused by burnup

With this fast forward algorithm the flux distribution after many time steps can be approximated by simple integrations (=summations) without having to solve the diffusion equation for every time step.

First however, the diffusion equation has to be solved once to obtain the initial flux distribution ϕ^0, and then for each cell c, the adjoint diffusion equation has to be solved. The final distribution is

$$\vec{N}^n = \exp\left(\mathbf{B}\left(\sum_{j=0}^{n-1}\phi^j\right)T\right)\vec{N}^0. \tag{5.1}$$

Now the resulting burnup can be calculated quickly from $\vec{N}^n$.

5.3 Backward flux calculations

Now we propose a backward algorithm, derived analogous to the forward one. We start with the desired nuclide densities at the end of the cycle ($\vec{N}^n$) and calculate what the beginning concentrations would be ($\vec{N}^0$). Therefore we describe the variations in the cross sections by

$$\delta\Sigma^i = \vec{\sigma}\cdot\left(\vec{N}^{i-1} - \vec{N}^i\right) \tag{5.2}$$

and the burnup equations 2.46 solved backward yield

$$\vec{N}^i = \exp\left(-\mathbf{B}\left(\sum_{j=i+1}^{n}\phi^j\right)T\right)\vec{N}^n. \tag{5.3}$$

So we get the following backward algorithm:

$\mathcal{B}$1. The final ($i = n$) nuclide density vector $\vec{N}^n$ is given. Now perform an eigenvalue calculation to obtain r^n (Section 2.3.3). The final cross sections are calculated with the equations of section 2.6. Then, the final flux distribution ϕ^n is found by solving the $1\frac{1}{2}$-group diffusion equation:

$$\nabla D^n \nabla\phi^n + \Sigma^n\phi^n = 0,$$

where

$$D^n = \frac{1}{3\Sigma^n_{tr}} \text{ and } \Sigma^n = \nu\Sigma^n_f - \Sigma^n_a - \Sigma^n_{a,\mathrm{ctrl}}.$$

$\mathcal{B}2$. For each fuel element c compute the adjoint ϕ_c^* described by

$$\nabla D^n \nabla \phi_c^* + \Sigma^n \phi_c^* = \begin{cases} -1 & \text{if} \quad (x,y) \in c \\ 0 & \text{if} \quad (x,y) \notin c \end{cases},$$

with boundary condition

$$2D^n \frac{\partial \phi_c^*}{\partial n} + \phi_c^* = \frac{-2 \int_c \phi^n \, dV}{\int_{\partial V} \phi^n \, dA}.$$

$\mathcal{B}3$. If $\bar{\phi}^i$ is a solution of the diffusion equation then $\eta\bar{\phi}^i$ is also a solution, so normalize the flux density $\bar{\phi}^i$ at the desired power level P (see eq. 2.9)

$$\eta = \frac{P}{\mu_f V_c \sum_c \vec{\sigma}_f \cdot \vec{N}^i(c) \bar{\phi}^i(c)}.$$

$\mathcal{B}4$. Calculate the nuclide density vector in period T_{i-1} ($\vec{N}^{i-1}$) and two quantities necessary to evaluate eq. 4.54: $\bar{\phi}^i_{\text{ctrl}}$, the flux caused by a unit variation ($\delta r = 1$) in the boric acid concentration and $\delta\bar{\phi}^i_{\text{burn}}$, the flux variation caused by the burnup:

$$\begin{aligned} \vec{N}^{i-1}(c) &= \exp\left(-\mathbf{B}\left(\bar{\phi}^i(c)\right) T\right) \vec{N}^i(c), \\ \bar{\phi}^i_{\text{ctrl}}(c) &= \sum_{c'} (\Sigma_{a,\text{B}} - \Sigma_{a,\text{mod}}) \bar{\phi}^i(c') \phi_c^*(c'), \\ \delta\bar{\phi}^i_{\text{burn}}(c) &= \sum_{c'} (\nu\vec{\sigma}_f - \vec{\sigma}_a) \cdot \left(\vec{N}^i(c') - \vec{N}^{i-1}(c')\right) \bar{\phi}^i(c') \phi_c^*(c'). \end{aligned}$$

$\mathcal{B}5$. Calculate the variation in the eigenvalue r as in eq. 4.56

$$\delta r^i = \frac{\sum_c \left[(\nu\vec{\sigma}_f - \vec{\sigma}_a) \cdot \left(\vec{N}^{i-1}(c) - \vec{N}^i(c)\right) \bar{\phi}^i(c)^2 \right]}{\sum_c \left[(\Sigma_{a,\text{B}} - \Sigma_{a,\text{mod}}) \bar{\phi}^i(c)^2 \right]}.$$

$\mathcal{B}6$. Compute the average flux density $\bar{\phi}^{i-1}$ in each fuel element c from the average flux densities in the latter periods $\left(\bar{\phi}^i, \ldots, \bar{\phi}^n\right)$ with eq. 4.54

$$\bar{\phi}^{i-1}(c) = \bar{\phi}^i(c) - \delta r^i \bar{\phi}^i_{\text{ctrl}}(c) - \delta\bar{\phi}^i_{\text{burn}}(c).$$

$\mathcal{B}7$. Let $i := i - 1$ and go to step $\mathcal{B}3$.

5.4 Implementation of the fast forward algorithm

We implemented the fast forward algorithm (FFA) in MatLab. The computer code can be found in appendix B.2. The finite differences method is used to approximate the differential equation by a matrix equation. (See section 3.1) So we get one matrix equation for the diffusion equation and C matrix equations with source term for the adjoint equations:

$$\begin{aligned} (\mathbf{A} - r\mathbf{I})\vec{\phi} &= \vec{0}, && (5.4) \\ (\mathbf{A}^* - r\mathbf{I})\vec{\phi}^*_c &= -\vec{Q}^*_c,\ c = 1, \ldots, C, && (5.5) \end{aligned}$$

with C the number of fuel elements. We choose $\vec{Q}^*_c$ in accordance with the forward algorithm: $\vec{Q}^*_c = \vec{e}_c$, the c^{th} elementary vector. So we can combine the ϕ^*_c's in a matrix Φ^*:

$$\begin{aligned} (\mathbf{A} - r\mathbf{I})\vec{\phi} &= \vec{0}, && (5.6) \\ (\mathbf{A}^* - r\mathbf{I})\Phi^* &= -\mathbf{I}. && (5.7) \end{aligned}$$

Now $\mathbf{A}$ contains the cross sections and when $\mathbf{A}$ is perturbed with $\delta\mathbf{A}$ and we get the following algorithm of section 5.2:

$$\vec{\phi}^{i+1} = (\mathbf{I} + \Phi^*(\delta\mathbf{A}^i - \delta r^i\mathbf{I}))\vec{\phi}^i = (\mathbf{I} + (\mathbf{A}^* - r\mathbf{I})^{-1}(\delta\mathbf{A}^i - \delta r^i\mathbf{I}))\vec{\phi}^i \qquad (5.8)$$

Chapter 6

Optimization results

The following strategy is used in the optimization:

1. Start with a known $\vec{N}^0$ for each fuel element. Combine all these vectors in a matrix $\mathbf{N^0}$.
2. Compute the initial flux density $\vec{\phi}^0$.
3. $\tilde{\mathbf{N}}_p^0$ is the p^{th} perturbation of $\mathbf{N}^0$ and with perturbation theorty compute $\tilde{\phi}_p^0$ and $\tilde{r}_p^0$.
4. Check whether the engineering constraints are met.
5. For each perturbation p use the forward algorithm to compute $\tilde{\mathbf{N}}_p^n$, $\tilde{\phi}_p^n$ and $\tilde{r}_p^n$.
6. For each perturbation p compute the objective function O_p.
7. Choose the perturbation p that maximizes the objective function O_p.

The perturbations of $\mathbf{N}^0$ have to be small, e.q. a binary exchange of fuel elements. So with this algorithm we can roughly examine the effect of these exchanges and choose the best p in step 6. With this best $\mathbf{N}_p^0$ we can start the algorithm again until no improvement is possible.

It is possible that the procedure described above will lead to a local extremum. Van Geemert [7] examined also higher order interchanges and found that the probability of getting stuck in a local extremum decreases with the order of the interchanges.

6.1 Comparisons of FFA with BoldVenture

To test my calculations I have done some control calculations with BoldVenture, a reliable neutron diffusion code. Two starting patterns of a 6×6 core with 3 age groups are considered. The lower right quarter of the pattern is shown.

3 2 3	3 3 2
2 2 1	3 2 1
3 1 1	2 1 1
pattern A	pattern B

Objective function II (see section 4.5) has been calculated for all possible binary exchanges with our Fast Forward Algorithm (FFA) and with BoldVenture. The results are shown in the figures 6.1 and 6.2. We see that FFA returns higher values than BoldVenture does. This is caused by the linearization in the FFA.

However, for pattern optimization we are not interested in the absolute value of the objective function, but in the variation of the objective function $O_p - O$. In the figures 6.3 and 6.4 these variations are compared for FFA and BoldVenture.

In the optimization process, one tries to find the permutation p with the highest possible improvement of the objective function. Figures 6.3 and 6.4 show that in these cases the FFA calculations yield the same choice of best permutation as the lengthy Boldventure calculations. (All lines connecting two points in figures 6.3 and 6.4 have positive slopes, except for one line connecting the two points in figure 6.4 with $O_p - O$ values near -0.05, which permutations are not interesting because pattern B itself is better.)

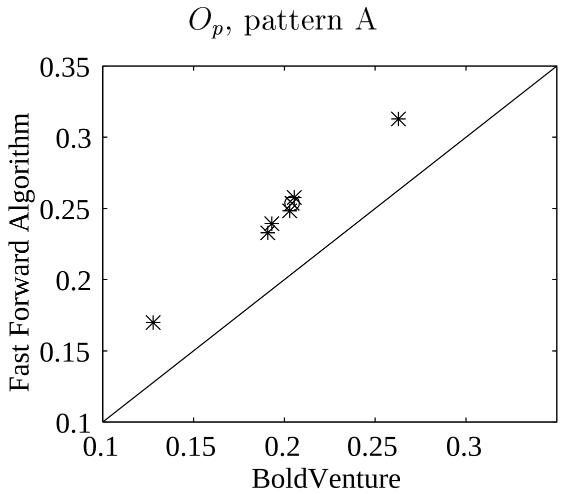

Figure 6.1: The objective O_p calculated with FFA and with BoldVenture for all possible permutations p of pattern A (pattern A itself is indicated by $\circ$)

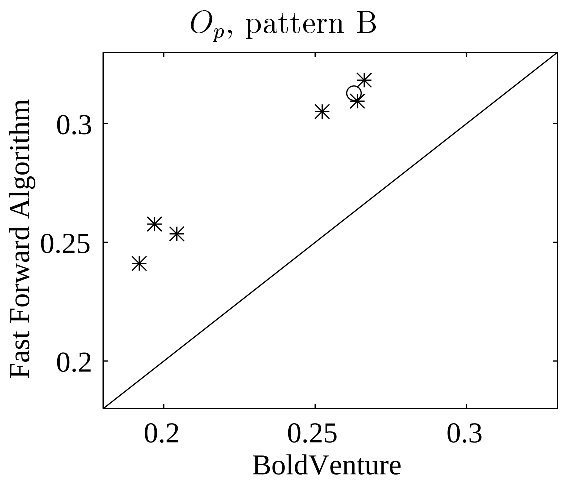

Figure 6.2: The objective O_p calculated with FFA and with BoldVenture for all possible permutations p of pattern B (pattern B itself is indicated by $\circ$)

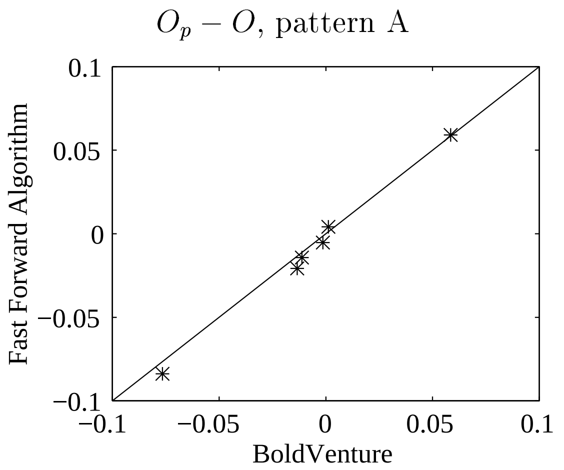

Figure 6.3: The variation of the objective function $O_p - O$ calculated with FFA and with BoldVenture compared for all possible permutations p of pattern A

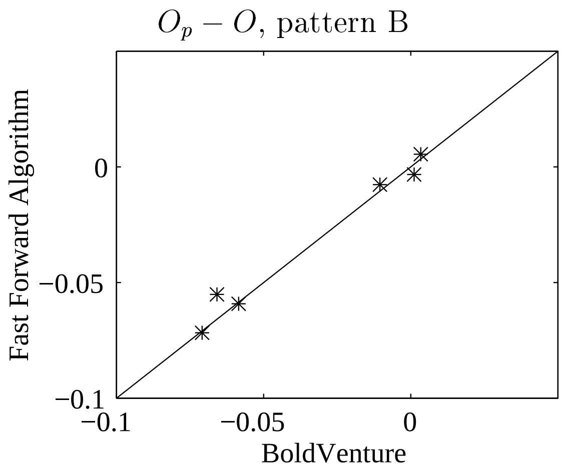

Figure 6.4: The variation of the objective function $O_p - O$ calculated with FFA and with BoldVenture compared for all possible permutations p of pattern B

6.2 Optimizations with FFA

In this section we optimized the reloading pattern for objective functions II and IV (see section 4.5). We consider again the lower right quarter of a square core with 6×6 elements and 3 age groups: fresh (1), older (2), and oldest (3).

Objective II ($\vec{N}^n$)

$$
\begin{array}{ccc}
 & \begin{array}{ccc} 2 & 2 & 3 \\ 2 & 1 & 1 \\ 3 & 1 & 3 \\ \hline \multicolumn{3}{c}{0.1712} \end{array} & \begin{array}{ccc} 1 & 2 & 3 \\ 2 & 3 & 1 \\ 3 & 1 & 2 \\ \hline \multicolumn{3}{c}{0.2255} \end{array} \\
 & \downarrow & \downarrow \\
 & \begin{array}{ccc} 2 & 3 & 2 \\ 3 & 1 & 1 \\ 2 & 1 & 3 \\ \hline \multicolumn{3}{c}{0.2487} \end{array} & \begin{array}{ccc} 1 & 3 & 2 \\ 3 & 3 & 1 \\ 2 & 1 & 2 \\ \hline \multicolumn{3}{c}{0.3070} \end{array} \\
 & \downarrow & \downarrow \\
\begin{array}{ccc} 3 & 2 & 3 \\ 2 & 2 & 1 \\ 3 & 1 & 1 \\ \hline \multicolumn{3}{c}{0.2536} \end{array} & \begin{array}{ccc} 3 & 3 & 2 \\ 3 & 1 & 1 \\ 2 & 1 & 2 \\ \hline \multicolumn{3}{c}{0.3095} \end{array} & \begin{array}{ccc} 1 & 3 & 1 \\ 3 & 3 & 2 \\ 1 & 2 & 2 \\ \hline \multicolumn{3}{c}{0.3118} \end{array} \\
\downarrow & \downarrow & \swarrow \\
\begin{array}{ccc} 3 & 3 & 2 \\ 3 & 2 & 1 \\ 2 & 1 & 1 \\ \hline \multicolumn{3}{c}{0.3128} \end{array} & \begin{array}{ccc} 3 & 3 & 1 \\ 3 & 1 & 2 \\ 1 & 2 & 2 \\ \hline \multicolumn{3}{c}{0.3161} \end{array} & \begin{array}{ccc} 1 & 3 & 1 \\ 3 & 2 & 2 \\ 1 & 2 & 3 \\ \hline \multicolumn{3}{c}{0.2564} \end{array} \\
\searrow & \downarrow & \swarrow \\
 & \begin{array}{ccc} 3 & 3 & 1 \\ 3 & 2 & 2 \\ 1 & 2 & 1 \\ \hline \multicolumn{3}{c}{0.3183} \end{array} &
\end{array}
$$

Objective IV (r^n)

$$
\begin{array}{ccc}
 & & \begin{array}{ccc} 3 & 2 & 3 \\ 2 & 2 & 1 \\ 3 & 1 & 1 \\ \hline \multicolumn{3}{c}{0.0288} \end{array} \\
 & & \downarrow \\
 & \begin{array}{ccc} 1 & 3 & 1 \\ 3 & 2 & 2 \\ 1 & 2 & 3 \\ \hline \multicolumn{3}{c}{0.0254} \end{array} & \begin{array}{ccc} 3 & 3 & 2 \\ 3 & 2 & 1 \\ 2 & 1 & 1 \\ \hline \multicolumn{3}{c}{0.0294} \end{array} \\
 & \downarrow & \\
\begin{array}{ccc} 2 & 2 & 3 \\ 2 & 1 & 1 \\ 3 & 1 & 3 \\ \hline \multicolumn{3}{c}{0.0287} \end{array} & \begin{array}{ccc} 3 & 3 & 1 \\ 3 & 2 & 2 \\ 1 & 2 & 1 \\ \hline \multicolumn{3}{c}{0.0293} \end{array} & \begin{array}{ccc} 1 & 2 & 3 \\ 2 & 3 & 1 \\ 3 & 1 & 2 \\ \hline \multicolumn{3}{c}{0.0230} \end{array} \\
\downarrow & \downarrow & \downarrow \\
\begin{array}{ccc} 2 & 3 & 2 \\ 3 & 1 & 1 \\ 2 & 1 & 3 \\ \hline \multicolumn{3}{c}{0.0294} \end{array} & \begin{array}{ccc} 3 & 3 & 1 \\ 3 & 1 & 2 \\ 1 & 2 & 2 \\ \hline \multicolumn{3}{c}{0.0297} \end{array} & \begin{array}{ccc} 3 & 2 & 3 \\ 2 & 1 & 1 \\ 3 & 1 & 2 \\ \hline \multicolumn{3}{c}{0.0292} \end{array} \\
\searrow & \downarrow & \swarrow \\
 & \begin{array}{ccc} 3 & 3 & 2 \\ 3 & 1 & 1 \\ 2 & 1 & 2 \\ \hline \multicolumn{3}{c}{0.0298} \end{array} &
\end{array}
$$

Figure 6.5: Several pattern optimizations for two objective functions

Several optimization paths are shown in figure 6.5. An arrow indicates one pair-wise interchange an is the best permutation found by FFA. The objective functions are printed below each pattern. As one can see, the optimal value of objective function II is 0.3183 and the optimal value of objective function IV is 0.0298. And these optimal patterns are found starting from 4 different starting patterns.

The graphical representations of the two optimal patterns are plotted in the figures 6.6 and 6.7. In both cases more than 10 starting patterns were used, all leading to the same optimal pattern. The lighter fuel elements are older. For a square core with 8×8 elements and 4 age groups the optimal patterns are plotted in the figures 6.8 and 6.9.

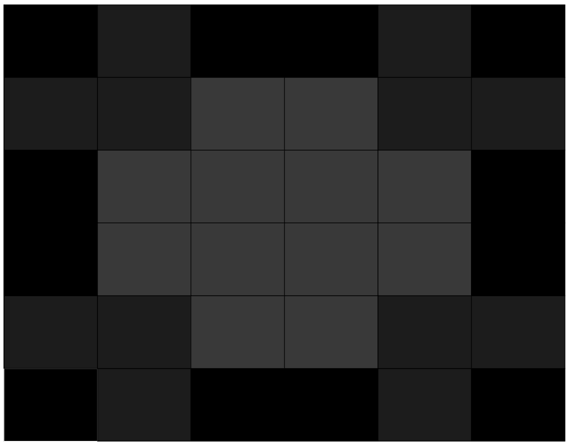

Figure 6.6: Optimal 6×6 pattern with objective function II

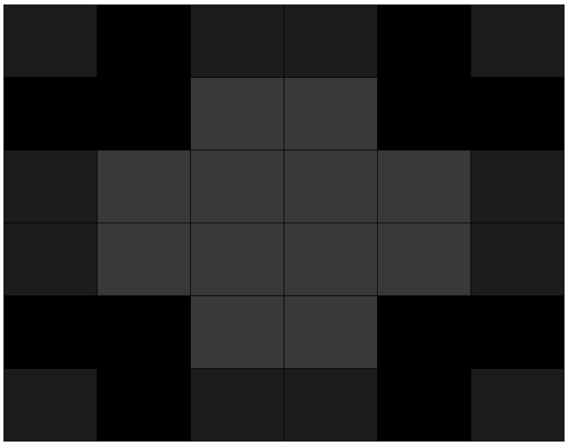

Figure 6.7: Optimal 6×6 pattern with objective function IV

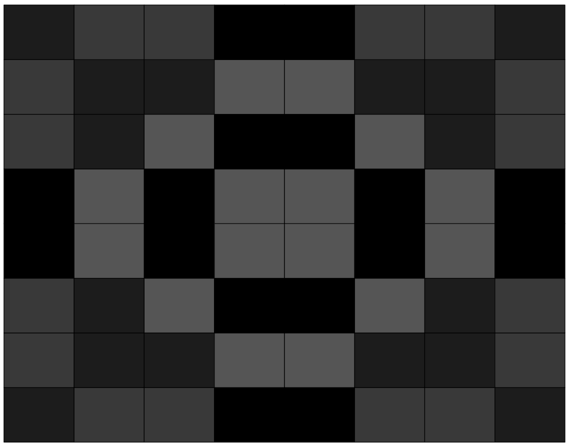

Figure 6.8: Optimal 8×8 pattern with objective function II

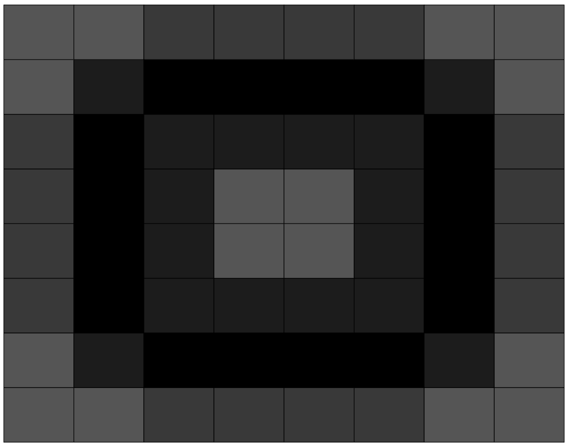

Figure 6.9: Optimal 8×8 pattern with objective function IV

6.3 Correlation between objective functions

To say something about the correlation of two objective functions we computed objective functions II, III and IV with FFA for a number of 8×8 reloading patterns with four age groups. The results are shown in the figures 6.10 and 6.11. The first plot shows that the

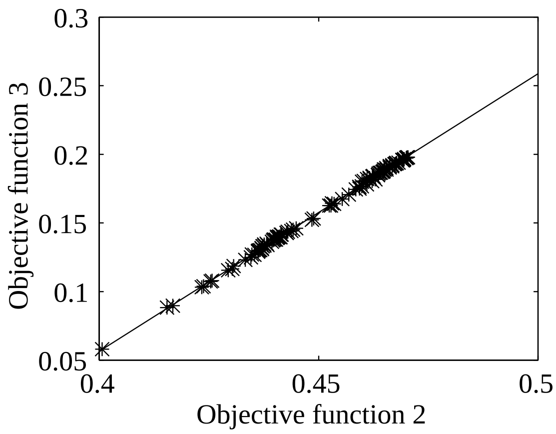

Figure 6.10: Correlation between objective function II and 3

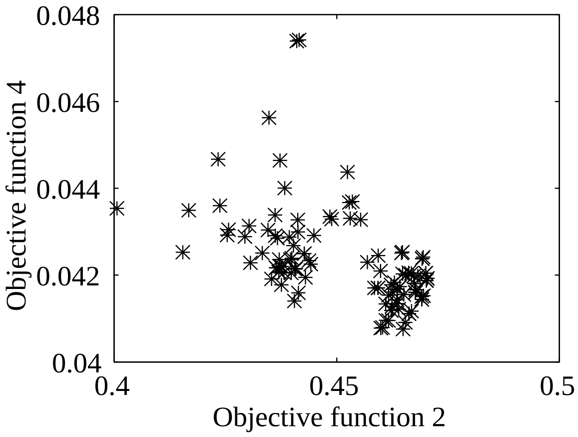

Figure 6.11: Correlation between objective function II and 4

correlation between objective function II and III is perfect. This means that the optimal pattern in the sense of objective function II is necessarily the optimal pattern in the sense of objective function III. Figure 6.11 shows that there is almost no correlation between objective function II and IV, only some 'clustering'. This agrees with section 6.2 where objective function II and IV yield different optimal patterns.

Conclusions

Validity FFA
The fast forward algorithm has been tested in a small number of cases against the standard code BoldVenture. In these cases the absolute value of the objective functions was not predicted well by the FFA. However, when several patterns are compared, FFA picks the same best pattern as BoldVenture does. So it seems that FFA can be used in optimization as long as small perturbations of the patterns are compared.

Time saving FFA
Suppose one wants to optimize the reloading pattern of a core with C fuel elements using a diffusion code like BoldVenture with n time steps. Then one needs to do $(P+1)n$ diffusion calculations, where P is the number of possible permutations. When binary exchanges are used, the number of possible permutations is $P = C(C-1)/2$. So the total number of diffusion calculations to find the optimal binary exchange is $(\frac{1}{2}C^2 - \frac{1}{2}C + 1)n$. If the Fast Forward Algorithm is used only 1 diffusion and C adjoint calculations are necessary. So FFA needs only $C+1$ diffusion calculations to find the optimal binary exchange. In table 6.1 the number of diffusion calculations is compared.

Objective functions, diffusion codes and optimization methods
The FFA has been developed and tested here with 4 representative objective functions, a finite difference solver, and one optimization method (best pair-wise interchange). The FFA is however applicable with other, similar objective functions, other solution methods for the diffusion equations, and with other optimization methods that compare several patterns that are not too different.

Table 6.1: Comparison of FFA and Boldventure

Number of fuel elements (C)	Number of diffusion calculations with n time steps	
	BoldVenture	FFA
4	$7n$	5
6	$16n$	7
10	$46n$	11
50	$1226n$	51

Bibliography

[1] Bell G.I. and Glasstone S., *Nuclear reactor theory*, Van Nostrand, New York, 1970.

[2] Chao J.A., Hu C.W. and Suo C.A., *A theory of fuel managment via backward diffusion calculation*, Nuclear Science and Engineering, **93**, pp. 78-87, 1986.

[3] Downar T.J. and Kim Y.J., *A reverse depletion method for pressurized water reactor core reload design*, Nuclear Technology, **73**, pp. 42-54, 1986.

[4] Duderstadt J.J. and Hamilton L.J., *Nuclear reactor analysis*, J. Wiley and Sons, New York, 1976.

[5] Gandini A., *Time-dependent generalized perturbation theory for burnup analysis*, CNEN RT/FI(75) 4, Comitato Nazionale per l' Energia Nucleare, Rome, 1975.

[6] Gandini A., Salvatores M., Tondinelli L., *New developments in generalized perturbation methods in the nuclide field*, Nuclear Science and Engineering, **62**, pp. 339-345, 1977.

[7] Geemert R. van, *Evaluation and optimization of fuel assembly shuffling schemes for a nuclear reactor core*, IRI-131-95-016, University of Technology Delft, 1995.

[8] Hoogenboom J.E., Dam H. van, *Kernreactorkunde*, Lecture notes c27, Delft, 1994.

[9] Jong A.J. de, *Reloading pattern design for batch refuelled nuclear reactors*, IRI-131-95-010, University of Technology Delft, 1995.

[10] Kan J. van, Segal A., *Numerieke methoden voor partiële differentiaalvergelijkingen*, Delftse Uitgevers Maatschappij, Delft, 1993.

[11] Mahlers Y.P., *Algorithms for solving some problems of the nuclear reactor optimiziation*, Annals of nuclear energy, Vol. 18, No. 11, pp. 661-664, 1991.

[12] Maldonado G.I., Turinsky P.J., *Application of nonlinear nodal diffusion generalized perturbation theory to nuclear fuel reload optimization*, Nuclear Technology, **110**, pp. 198-219, 1995.

[13] Marchuk G.I., *Adjoint equations and analysis of complex systems*, Kluwer Academic Publishers, Dordrecht, 1995.

[14] Marchuk G.I., *Numerical methods for nuclear reactor calculations*, Consultants Bureau, New York, 1959.

[15] Marchuk G.I. and Lebedev V.I., *Numerical methods in the theory of neutron transport*, Harwood Academic Publishers, Amsterdam, 1986.

[16] Internet, several sites (see appendix A)

[17] Suzuki A. and Kiyose R., *Maximizing the average fuel burnup over entire core: a Poison managment optimization problem for multizone light-water reactor cores* Nuclear Science and Engineering, **44**, pp. 121-134, 1971.

[18] Vroegindeweij C., *Generalized perturbation theory*, ECN-I-92-034, Petten, 1992.

[19] Weaver L.E., *Reactor dynamics and control*, Elsevier, New York, 1968.

[20] Williams M.L., *Development of depletion perturbation theory for coupled neutron/nuclide fields*, Nuclear Science and Engineering, **70**, pp. 20-36, 1979.

[21] Yang W.S. and Downar T.J., *Generalized perturbation theory for constant power core depletion*, Nuclear Science and Engineering, **99**, pp. 353-366, 1988.

[22] Zhian L. and Levine S.H., *Autoload, an automatic optimal pressurized water reactor reload design system with an expert module*, Nuclear Science and Engineering, **118**, 67-78, 1994.

Appendix A

Nuclear technology and the Internet

The internet is a large computer network all over the world. It connects several billions of computers with each other and all kind of information can be accessed accurately and there is also a lot about nuclear technology. So, if you need nuclear data you can access the National Nuclear Data Center (NNDC), or, if you're interested in the radioactive waste program of the U.S. you can find it at the NRC home page. For those interested, here are some sites with a lot of valuable information:

Virtual Library [Nuclear Engineering]:
http://neutrino.nuc.berkeley.edu/NEadm.html
Natinoal Nuclear Data Center:
http://datwww.dne.bnl.gov/nndc.html
U.S. Department of Energy:
http://www.esd.ornl.gov/doe-labs/doe-labs.html
Nuclear Regulatory Commission:
http://www.nrc.gov/
Uranium Information Centre:
http://www.uic.com.au/

For example, at the NRC-site plant information books for more than a hundred commercial nuclear power plants are available. The information includes facility statistics, emergency response information, plant description summary, simplified plant system diagrams, detailed plant system data, and so on. To give you an impression I collected some information and plots about the Turkey Point Reactors.

A.1 The Turkey Point Unit 4

A.1.1 General information

Plant Name:	Turkey Point Unit 4
Docket No.:	50-251
Owner/Operator:	Florida Power & Light Co.

Other Plants On Site:	Turkey point Unit 1/Unit 2 (Oil & gas fired) and Turkey Point Unit 3 (Nuclear)
Site Location/Address:	Situated on Biscayne Bay about 25 miles south of Miami, FL
Facility Licensed Thermal Power Limit:	(Ref: License) 2200 MWt
Main Turbine Generator Rated Output:	760 MWe
PWR Type:	3-loop (see figure A.1)
NSSS Vendor:	Westinghouse
Turbine Generator:	Westinghouse
Arch. Engr.:	Bechtel Corporation
Constructor:	Bechtel Corporation
Date of Operating License Issuance:	04/10/73
Date of Commercial Operation:	09/07/73

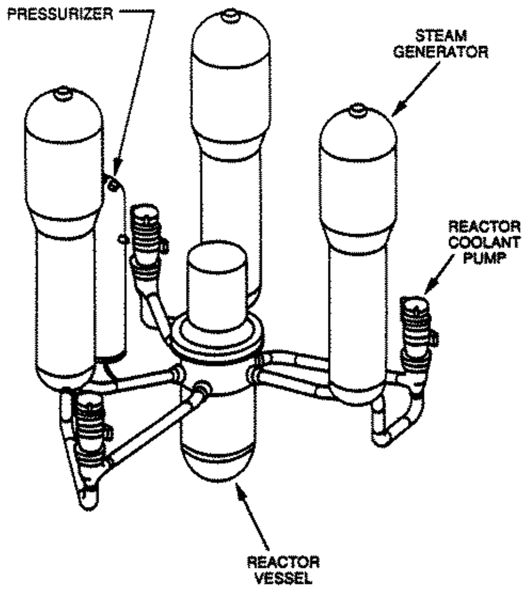

Figure A.1: Three loop reactor system

A.1.2 Plant summary

Containment	
Containment Type:	Large Dry
Design Pressure:	55 psig
Steam Generator	
Steam Generator Model:	44F
Number of Steam Generators:	3
Number of Main Steam Isolation Valves:	3
Fuel	
No. of Fuel Assemblies:	157
No. of Fuel Rods per Assembly:	204($= 15 \times 15 - 21$ burnable poison)

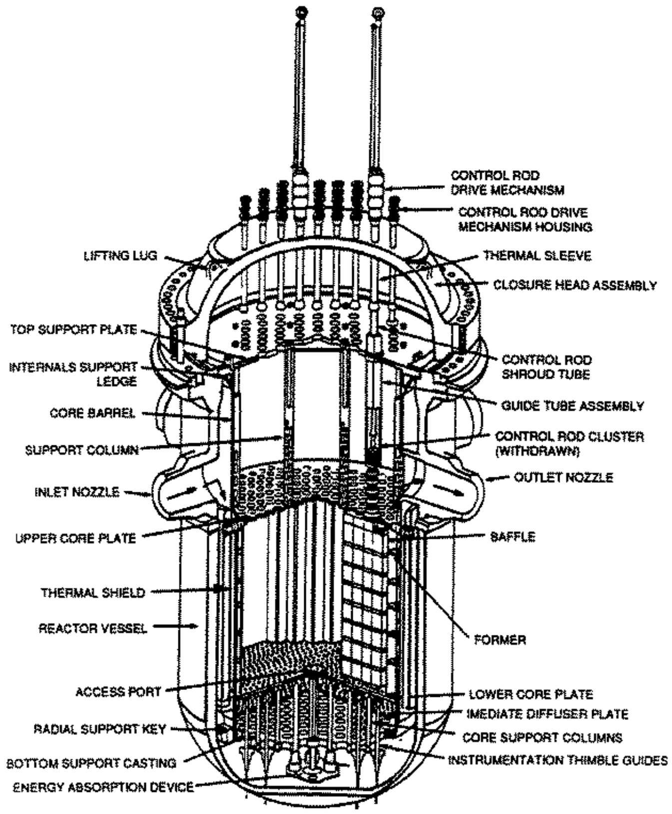

Figure A.2: Reactor vessel internals

Appendix B

Computer code

B.1 BoldVenture

```
=CONTROL1
TEST BURN-UP OPTION
999999     0     0     0    10    50     0     0     0   0   0   0   0   0   0
  1  2  2  7 13
END
USE INPUT PROCESSOR TO GENERATE GRUPXS FILE
 0V GRUPXS *HGBM test* 1     $ 2 group 16 nucl
 1D 2 16 1 1 0 1 176 0 0 0 1 1 0 0
 2D *THIS IS A TEST                                         *
    *Zr    I135  Xe135 Cs135 Pm149 Sm149 U235  U238  Pu239 Pu240 *
    *Pu241 Pu242 Am241 Hy    O16F  O16M  *
    1. 0. 1.74E+7  4.15E+5   1.96E+7 0.625  1.E-5

(...BODY AVAILABLE AT IRI...)

REFINS        0 20  0 20  1
         0.0        0.25      5.0E+6     0.33333     1.3E-09          0.1
        0.15


  0


END
```

B.2 MatLab

```
clear;
hold off;
diary adj.out
flops(0);
tic;

%Constants and pre-definitions
q=1;                    %Convergence factor
c=3;                    %Size of the core
nage=3;                 %Number of age groups
nu=2.6;                 %Number of neutrons per fission
l=7;                    %Width of the elements
T=60*60*24*14/q;        %Length of time interval
P=2.5*10^6;             %Power
muf=10^(-12);           %Energy per fission
h=10;                   %Length of the elements
A=zeros(c^2,c^2);

%Microscopic cross sections for three nuclides (235, 238, 239)
sf(1)=1.29*10^(-24);sf(2)=0.215*10^(-24);sf(3)=1.50*10^(-24);
str(1)=6.8*10^(-24);str(2)=6.9*10^(-24);str(3)=6.50*10^(-24);
sa(1)=1.50*10^(-24);sa(2)=0.327*10^(-24);sa(3)=2.00*10^(-24);

%Initial nuclide density
age=[[6 8 9];           %Fresh
     [2 4 5];           %Older
     [1 3 7]];          %Oldest
for i=1:c^2/nage;
  N0(1,age(1,i))=0.04545*10^(24);
  N0(1,age(2,i))=0.04040*10^(24);
  N0(1,age(3,i))=0.03535*10^(24);
end;
N0(2,:)=0.00256*10^(24)*ones(1,c^2);
N0(3,:)=0.00000*10^(24)*ones(1,c^2);
U=[2 3 6];                             %Upper half
R=[3 6 9 7 8 9];                       %Boundary
Tot=[1 0 0]*N0*ones(c^2,1);
Sbmod=1;
Ovector=ones(c^2,1);                   %Optimization vector
for k=1:nage;
  %Ovector(age(nage,k))=1-nage;        %Objective function III
  Ovector(age(nage,k))=-1;             %Objective function II
```

```
end;

%Possible permutations
i=1;
%U<->U permutations
for a=1:c*(c-1)/2;
  for b=a+1:c*(c-1)/2;
    pm(i,1)=U(a);
    pm(i,2)=U(b);
    pm(i,3)=1+floor((U(a)-1)/c)+c*(U(a)-1-c*floor((U(a)-1)/c));
    pm(i,4)=1+floor((U(b)-1)/c)+c*(U(b)-1-c*floor((U(b)-1)/c));
    i=i+1;
  end;
end;
%D<->D permutations
for a=1:c;
  for b=a+1:c;
    pm(i,1)=1+(a-1)*(c+1);
    pm(i,2)=1+(b-1)*(c+1);
    pm(i,3)=1+(a-1)*(c+1);
    pm(i,4)=1+(b-1)*(c+1);
    i=i+1;
  end;
end;
%D<->U permutations
for a=1:c;
  for b=1:c*(c-1)/2;
    for aa=a+1:c;
      pm(i,1)=1+(a-1)*(c+1);
      pm(i,2)=U(b);
      pm(i,3)=1+(aa-1)*(c+1);
      pm(i,4)=1+floor((U(b)-1)/c)+c*(U(b)-1-c*floor((U(b)-1)/c));
      i=i+1;
    end;
  end;
end;
pm(i,1)=1;pm(i,2)=1;pm(i,3)=1;pm(i,4)=1;
n=i;

%Examine binary exchanges
Optimaal=1;
Next=eye(c^2);
while pm(Optimaal,1)~=pm(Optimaal,2);
  for a=1:c;
```

```
  for b=1:c;
    Nmat(a,b)=N0(1,(a-1)*c+b);
  end;
end;
disp(round((0.0505*ones(c,c)-Nmat*10^(-24))/0.00505));


%Definition matrix
A(1,1)=-2/(Str(1)+Str(2))-2/(Str(1)+Str(1+c))
 +3*l^2*(nu*Sf(1)-Sa(1));
A(1,2)=2/(Str(1)+Str(2));
A(1,1+c)=2/(Str(1)+Str(1+c));

A(c,c-1)=2/(Str(c)+Str(c-1));
A(c,c)=-2/(Str(c)+Str(c-1))-2/(Str(c)+Str(2*c))
 -1/Str(c)+1/Str(c)*(8-6*l*Str(c))/(8+6*l*Str(c))
 +3*l^2*(nu*Sf(c)-Sa(c));
A(c,2*c)=2/(Str(c)+Str(2*c));

A((c-1)*c+1,(c-2)*c+1)=2/(Str((c-1)*c+1)+Str((c-2)*c+1));
A((c-1)*c+1,(c-1)*c+1)=-2/(Str((c-1)*c+1)+Str((c-2)*c+1))
 -2/(Str((c-1)*c+1)+Str((c-1)*c+2))-1/Str((c-1)*c+1)
 +1/Str((c-1)*c+1)*(8-6*l*Str((c-1)*c+1))/(8+6*l*Str((c-1)*c+1))
 +3*l^2*(nu*Sf((c-1)*c+1)-Sa((c-1)*c+1) );
A((c-1)*c+1,(c-1)*c+2)=2/(Str((c-1)*c+1)+Str((c-1)*c+2));

A(c^2,c^2-c)=2/(Str(c^2)+Str(c^2-c));
A(c^2,c^2-1)=2/(Str(c^2)+Str(c^2-1));
A(c^2,c^2)=-2/(Str(c^2)+Str(c^2-c))-2/(Str(c^2)+Str(c^2-1))
 -2/Str(c^2)+2/Str(c^2)*(8-6*l*Str(c^2))/(8+6*l*Str(c^2))
 +3*l^2*(nu*Sf(c^2)-Sa(c^2));

for a=2:c-1;
  A(a,a-1)=2/(Str(a)+Str(a-1));
  A(a,a)=-2/(Str(a)+Str(a-1))-2/(Str(a)+Str(a+1))
   -2/(Str(a)+Str(a+c))+3*l^2*(nu*Sf(a)-Sa(a));
  A(a,a+1)=2/(Str(a)+Str(a+1));
  A(a,a+c)=2/(Str(a)+Str(a+c));

  A((a-1)*c+1,(a-2)*c+1)=2/(Str((a-1)*c+1)+Str((a-2)*c+1));
  A((a-1)*c+1,(a-1)*c+1)=-2/(Str((a-1)*c+1)+Str((a-2)*c+1))
   -2/(Str((a-1)*c+1)+Str((a-1)*c+2))-2/(Str((a-1)*c+1)+Str(a*c+1))
   +3*l^2*(nu*Sf((a-1)*c+1)-Sa((a-1)*c+1));
  A((a-1)*c+1,(a-1)*c+2)=2/(Str((a-1)*c+1)+Str((a-1)*c+2));
```

```
  A((a-1)*c+1,a*c+1)=2/(Str((a-1)*c+1)+Str(a*c+1));

  A(a*c,(a-1)*c)=2/(Str(a*c)+Str((a-1)*c));
  A(a*c,a*c-1)=2/(Str(a*c)+Str(a*c-1));
  A(a*c,a*c)=-2/(Str(a*c)+Str((a-1)*c))-2/(Str(a*c)+Str(a*c-1))
   -2/(Str(a*c)+Str((a+1)*c))-1/Str(a*c)
   +1/Str(a*c)*(8-6*l*Str(a*c))/(8+6*l*Str(a*c))
   +3*l^2*(nu*Sf(a*c)-Sa(a*c));
  A(a*c,(a+1)*c)=2/(Str(a*c)+Str((a+1)*c));

  A((c-1)*c+a,(c-2)*c+a)=2/(Str((c-1)*c+a)+Str((c-2)*c+a));
  A((c-1)*c+a,(c-1)*c+a-1)=2/(Str((c-1)*c+a)+Str((c-1)*c+a-1));
  A((c-1)*c+a,(c-1)*c+a)= -2/(Str((c-1)*c+a)+Str((c-2)*c+a))
   -2/(Str((c-1)*c+a)+Str((c-1)*c+a-1))
   -2/(Str((c-1)*c+a)+Str((c-1)*c+a+1))-1/Str((c-1)*c+a)
   +1/Str((c-1)*c+a)*(8-6*l*Str((c-1)*c+a))/(8+6*l*Str((c-1)*c+a))
   +3*l^2*(nu*Sf((c-1)*c+a)-Sa((c-1)*c+a));
  A((c-1)*c+a,(c-1)*c+a+1)=2/(Str((c-1)*c+a)+Str((c-1)*c+a+1));
end;

for a=2:c-1;
  for b=2:c-1;
    A((a-1)*c+b,(a-2)*c+b)=2/(Str((a-1)*c+b)+Str((a-2)*c+b));
    A((a-1)*c+b,(a-1)*c+b-1)=2/(Str((a-1)*c+b)+Str((a-1)*c+b-1));
    A((a-1)*c+b,(a-1)*c+b)=-2/(Str((a-1)*c+b)+Str((a-2)*c+b))
     -2/(Str((a-1)*c+b)+Str((a-1)*c+b-1))
     -2/(Str((a-1)*c+b)+Str((a-1)*c+b+1))
     -2/(Str((a-1)*c+b)+Str(a*c+b))
     +3*l^2*(nu*Sf((a-1)*c+b)-Sa((a-1)*c+b));
    A((a-1)*c+b,(a-1)*c+b+1)=2/(Str((a-1)*c+b)+Str((a-1)*c+b+1));
    A((a-1)*c+b,a*c+b)=2/(Str((a-1)*c+b)+Str(a*c+b));
  end;
end;

%Calculation eigenvalue
[V,D]=eig(A);
[pos,pos]=find(D==max(max(D)));
phi0=V(:,pos);
r0=D(pos,pos)/(3*l^2*Sbmod);

%Calculation adjoint
%phirand=0;
%for k=1:2*c
%  phirand=phirand+(1+(8-6*l*Str(R(k)))/
```

```
%  (8+6*l*Str(R(k))))*phi(R(k))/2;
%end;
%phirand=4*phirand;
DD=zeros(c^2,c^2);
for k=1:2*c
  DD(R(k),R(k))=DD(R(k),R(k))-3*l^2*Str(R(k));
  %DD(R(k),R(k))=DD(R(k),R(k))+12*l/(8+6*l*Str(R(k)))
  %*(-2*l*phi(R(k)))/phirand;
end;
adj0=(A-3*l^2*Sbmod*r*eye(c^2,c^2)+DD)^(-1);
%pause

for i=1:n;
  if ((N0(1,pm(i,1))==N0(1,pm(i,3)))
    &(N0(1,pm(i,1))~=N0(1,pm(i,2))))|(i==n);
    Pm=eye(c^2);
    Pm(pm(i,1),pm(i,1))=0;
    Pm(pm(i,2),pm(i,2))=0;
    Pm(pm(i,1),pm(i,2))=1;
    Pm(pm(i,2),pm(i,1))=1;
    Pm(pm(i,3),pm(i,3))=0;
    Pm(pm(i,4),pm(i,4))=0;
    Pm(pm(i,3),pm(i,4))=1;
    Pm(pm(i,4),pm(i,3))=1;

    %Permute N
    N=N0*Pm;

    %Calculation macroscopic cross sections
    Str=str*N;
    Sf=sf*N;
    Sa=sa*N;

    r=r0+(((nu*sf-sa)*(N-N0))*phi2)/(Sbmod*sum(phi2));
    deltaA=zeros(c^2,c^2);
    for k=1:c^2
      deltaA(k,k)=3*l^2*((nu*sf-sa)*(N(:,k)-N0(:,k))
      -(r-r0)*Sbmod);
    end;
    phi=phi0-adj0*deltaA*phi0;

    %Loop over time
    j=1;
    phipos=1;
```

```
while (j<=26*q)&(r(j)>0) %&(phipos==1)

  %Normalization
  eta=P/(muf*h*l^2*Sf*phi);
  phi=eta*phi;

  %Burnup calculation
  B=zeros(3,3);
  phi2=zeros(c^2,1);
  for k=1:c^2
    B(1,1)=exp(-sa(1)*phi(k)*T);
    B(2,2)=exp(-(sa(2)-sf(2))*phi(k)*T);
    B(3,2)=(sa(2)-sf(2))/(sa(3)-(sa(2)-sf(2)))*(exp(-(sa(2)-sf(2))
          *phi(k)*T)-exp(-sa(3)*phi(k)*T));
    B(3,3)=exp(-sa(3)*phi(k)*T);
    Nnw(:,k)=B*N(:,k);
    %disp([Nnw(:,k) N(:,k)]);
    phi2(k)=phi(k)^2;
  end;

  %Eigenvalue calculation
  r(j+1)=r(j)+(((nu*sf-sa)*(Nnw-N))*phi2)/(Sbmod*sum(phi2));
  %disp([r(j+1) r(j)]);


  deltaA=zeros(c^2,c^2);
  for k=1:c^2
    deltaA(k,k)=3*l^2*((nu*sf-sa)*(Nnw(:,k)-N(:,k))
    -(r(j+1)-r(j))*Sbmod);
  end;

  %Flux calculation
  phi=phi-adj*deltaA*phi;
  for k=1:c^2;
    if phi(k)<0
      phipos=-1;
    end;
  end;

  N=Nnw;
  j=j+1;
end;

if j>=26*q;
```

```
      Objective(i)=([1 0 0]*N)*(Pm*Next*Ovector)/Tot;
      %Objective(i)=r(j);
      disp(['Exchange no. ' num2str(i) ': ' num2str(Objective(i))]);
    else
      Objective(i)=0;
      disp(['Exchange no. ' num2str(i) ': Engineering constraint']);
    end;
    if Objective(i)==max(Objective(:,1:i))
      Pmsave=Pm;
    end;

    %Plot final flux distribution and eigenvalue
    %F=[[phi(1),phi(2),phi(3)];
        [phi(4),phi(5),phi(6)];
        [phi(7),phi(8),phi(9)]];
    %F=[fliplr(flipud(F)) flipud(F); fliplr(F) F];
    %colormap([1 1 1]);
    %surf(F);
    %pause;
    %if i==n
      %plot((1:j)*T,r)
      %xlabel('time')
      %ylabel('r')
      %text(j*T,r(j),num2str(Objective(i)));
      %hold on;
      %print -dps rtime.ps
      %pause
    %end;
  else
    Objective(i)=0;
    disp(['Exchange no. ' num2str(i) ': Same or asymmetric pattern']);
  end;
end;

Optimaal=find(Objective==max(Objective));
Optimaal=Optimaal(1);
disp('Optimal binary exchange:')
if pm(Optimaal,1)~=pm(Optimaal,2)
  disp([' ' num2str(pm(Optimaal,1)) ' <-> ',num2str(pm(Optimaal,2))])
else
  disp([' Optimum reached: ' num2str(Objective(n))]);
end;
if pm(Optimaal,3)~=pm(Optimaal,4)
  disp([' ' num2str(pm(Optimaal,3)) ' <-> ',num2str(pm(Optimaal,4))])
```

```
  end;
  if pm(Optimaal,1)~=pm(Optimaal,2)
    disp(['Objective: ' num2str(Objective(n))
    ' -> ' num2str(max(Objective))]);
  end;

  N0=N0*Pmsave;
  Next=Pmsave*Next;
end;

t=toc
megaflops=flops/t/1.e6
diary off

%Plot optimal pattern
for a=1:c;
  for b=1:c;
    Nmat(a,b)=N0(1,(a-1)*c+b);
  end;
end;
Nmat=[fliplr(flipud(Nmat)) flipud(Nmat); fliplr(Nmat) Nmat];
Nmat=[[Nmat zeros(2*c,1)];zeros(1,2*c+1)];
pcolor(Nmat)
axis('off');
colormap(ones(10,3)-1.0*gray(10))
view([0 0 1])
```